

# AGARD

ADVISORY GROUP FOR AEROSPACE RESEARCH & DEVELOPMENT

7 RUE ANCELLE 92200 NEUILLY SUR SEINE FRANCE

AGARDograph No. 162

on

## Acoustic Fatigue Design Data

Part II

by

A.G.R. Thomson and R.F. Lambert

PROPERTY OF  
TECHNICAL LIBRARY  
P32-01

**BOEING VERTOL COMPANY**  
A DIVISION OF THE BOEING COMPANY

FORM 52920 (6/73)

ATLANTIC TREATY ORGANIZATION



DISTRIBUTION AND AVAILABILITY  
ON BACK COVER

NORTH ATLANTIC TREATY ORGANIZATION  
ADVISORY GROUP FOR AEROSPACE RESEARCH AND DEVELOPMENT  
(ORGANISATION DU TRAITE DE L'ATLANTIQUE NORD)

AGARDograph 162  
ACOUSTIC FATIGUE DESIGN DATA  
Part II

by

A.G.R.Thomson and R.F.Lambert  
Engineering Sciences Data Unit Ltd  
London, UK

LIBRARY  
VER 780450  
JUN - 6 1978  
BOEING - VERTOL

## THE MISSION OF AGARD

The mission of AGARD is to bring together the leading personalities of the NATO nations in the fields of science and technology relating to aerospace for the following purposes:

- Exchanging of scientific and technical information;
- Continuously stimulating advances in the aerospace sciences relevant to strengthening the common defence posture;
- Improving the co-operation among member nations in aerospace research and development;
- Providing scientific and technical advice and assistance to the North Atlantic Military Committee in the field of aerospace research and development;
- Rendering scientific and technical assistance, as requested, to other NATO bodies and to member nations in connection with research and development problems in the aerospace field.
- Providing assistance to member nations for the purpose of increasing their scientific and technical potential;
- Recommending effective ways for the member nations to use their research and development capabilities for the common benefit of the NATO community.

The highest authority within AGARD is the National Delegates Board consisting of officially appointed senior representatives from each Member Nation. The mission of AGARD is carried out through the Panels which are composed for experts appointed by the National Delegates, the Consultant and Exchange Program and the Aerospace Applications Studies Program. The results of AGARD work are reported to the Member Nations and the NATO Authorities through the AGARD series of publications of which this is one.

Participation in AGARD activities is by invitation only and is normally limited to citizens of the NATO nations.

The material in this publication has been reproduced directly from copy supplied by AGARD or the author.

Published November 1972

620.178.3



*Printed by Technical Editing and Reproduction Ltd  
Harford House, 7-9 Charlotte St, London. W1P 1HD*

## PREFACE

This volume, the second part of a series giving data for design against acoustic fatigue, has been prepared in order to draw together the results of research in acoustic fatigue and to present them in a form directly useable in aerospace design. Future work in this series will deal with endurance of titanium alloy structures under simulated acoustic loading, near field compressor noise estimation, stress response of box and control surface structures, structural damping and stress response of skin-stringer panels with stringers of relatively low flexural stiffness.

The AGARD Structures and Materials Panel has for many years been active in encouraging and coordinating the work that has been necessary to make this collection of design data possible and after agreeing on procedures for the acquisition, analysis and interpretation of the requisite data, work on this series of design data sheets was initiated in 1970.

The overall management of the project has been conducted by the Working Group on Acoustic Fatigue of the AGARD Structures and Materials Panel, and the project has been financed through a collective fund established by the Nations collaborating in the project, namely Canada, France, Germany, Italy, U.K. and U.S. National Coordinators appointed by each country have provided the basic data, liaised with the sources of the data, and provided constructive comment on draft data sheets. These Coordinators are Dr G.M. Lindberg (Canada), Mr R. Loubet (France), Mr G. Bayerdörfer (Germany), Gen. A. Griselli (Italy), Mr N.A. Townsend (U.K.), Mr A.W. Kolb (U.S.) and Mr F.F. Rudder (U.S.). Staff of the Engineering Sciences Data Unit Ltd, London, have analysed the basic data and prepared and edited the resultant data sheets with invaluable guidance and advice from the National Coordinators and from the Acoustic Fatigue Panel of the Royal Aeronautical Society which has the following constitution: Professor B.L. Clarkson (Chairman), Mr D.C.G. Eaton, Mr J.A. Hay, Mr W.T. Kirkby, Mr M.J.T. Smith and Mr N.A. Townsend. The members of Staff of the Engineering Sciences Data Unit concerned with the preparation of the data sheets in this volume are: Mr A.G.R. Thomson (Executive, Environmental Projects), Dr G. Sen Gupta and Mr R.F. Lambert (Environmental Projects Group).

Data sheets based on this AGARDograph will subsequently be issued in the Fatigue Series of Engineering Sciences Data issued by ESDU Ltd, where additions and amendments will be made to maintain their current applicability.



A.H. Hall  
Chairman,  
Working Group on Acoustic Fatigue  
Structures and Materials Panel

## CONTENTS

		<u>Page No.</u>
SECTION 1.	ENDURANCE OF ALUMINIUM ALLOY STRUCTURAL ELEMENTS SUBJECTED TO SIMULATED ACOUSTIC LOADING	
1.1	Notation	1
1.2	Notes	1
1.3	Plain Test Specimens	2
1.4	Integrally Machined Test Specimens	2
1.5	Riveted-Skin Test Specimens	3
1.6	Rib-Flange Test Specimens	4
1.7	Derivation and References	4
Figures		6
APPENDIX		
1A	Materials	17
SECTION 2.	NATURAL FREQUENCIES OF FLAT OR SINGLY-CURVED SANDWICH PANELS WITH CORES OF ZERO FLEXURAL STIFFNESS	
2.1	Notation	19
2.2	Notes	20
2.3	Derivation and References	21
2.4	Example	22
Figures		23
SECTION 3.	STRESS RESPONSE OF FLAT OR SINGLY-CURVED SANDWICH PANELS WITH CORES OF ZERO FLEXURAL STIFFNESS SUBJECTED TO RANDOM ACOUSTIC LOADING	
3.1	Notation	28
3.2	Notes	29
3.3	Calculation Procedure	29
3.4	Comparison with Measured Data	30
3.5	Derivation and References	31
3.6	Example	32
Figures		35
APPENDIX		
3A	Computer Program	51

## Section 1

ENDURANCE OF ALUMINIUM ALLOY STRUCTURAL ELEMENTS  
SUBJECTED TO SIMULATED ACOUSTIC LOADING1.1 Notation

$S_{rms}$	root mean square value of stress at a reference position	$N/m^2$	$lbf/in^2$
$N_r$	equivalent endurance	cycles	cycles

1.2 Notes

This Section gives the results of fatigue tests on aluminium alloy specimens, typical of aircraft structural components, excited by narrow band random loading to simulate acoustic fatigue loading. The results are presented in the form of curves of  $S_{rms}$  against  $N_r$ , where  $S_{rms}$  is the root mean square stress of the stress-time function and  $N_r$  is taken as half the number of zero crossings to failure of the stress-time function.

Data for four types of specimen are presented, i.e. plain, integrally-machined, riveted-skin and rib-flange specimens. The data are for specimens tested under reversed bending loading which produced a random amplitude stress distribution about a zero mean stress. The materials used are identified by the designation given in the test report, and the material type and the equivalent United States specification can be identified from the material description given in Appendix 1A.

All data presented are for aluminium-copper alloys. Test data for aluminium-zinc alloys are available but are not presented because their crack propagation rate is greater than for aluminium-copper alloys rendering them less suitable for use in an acoustic environment. The lives for the two types of alloy are however similar. Aluminium-zinc alloys that are given a two stage precipitation heat treatment intended to improve their resistance to crack propagation are manufactured but acoustic fatigue data for these materials are not yet available.

On the Figures of  $S_{rms}$  against  $N_r$  for the various types of construction, material and jointing compound, the test points plotted represent mean nominal stresses over the areas covered by the strain gauges. In the absence of data beyond  $10^9$  cycles a least-squares fitted straight line has been drawn through the test points. It is expected that test points beyond  $10^9$  cycles would generally lie above this line. The lines drawn through the test data are given for guidance only and should not be used directly for design because when estimating life due account should be taken of scatter in test data.

Two types of viscoelastic jointing compound were used in the riveted-skin and rib-flange tests. Using type 1 jointing compound there was no strong bond between mating surfaces, but type 2 compound created a strong bond between the mating skin and flange surfaces. The effect of the jointing compounds on the position of failure of the riveted skin test specimens is shown in Figures 1.14 and 1.15, and the effect on the stress distribution across the skin is shown in Figure 1.16. A notable feature of the effect of a type 2 viscoelastic jointing compound on a test specimen having a single row of skin attachment rivets is that the rivet line root mean square stress developed in such a specimen is considerably less than that developed in specimens having dry joints or joints with type 1 jointing compound for the same level of input force.

A comparison of S-N curve data for riveted-skin specimens with and without the viscoelastic jointing compounds shows that the endurance is little affected by the jointing compound. However, apart from the possible redistribution of stress, there is an advantage in using a viscoelastic jointing compound, in that for a given exciting force the stress level is less because of the increase in damping.

In Figure 1.3 the effect of surface cladding is evident. The endurance for clad material is less than for similar material in the unclad state; however, this difference is greater on plain specimens than on notched specimens, and is further reduced where fretting takes place.

The range of response frequencies for the riveted-skin and rib-flange tests is indicated on the Figures of S-N data. Over the range of frequency of interest (100-1000Hz) no effect of frequency on the endurance of the specimens was identified.

A limited number of the tests on skins attached by double rows of rivets were carried out at a temperature of  $-40^{\circ}\text{C}$ . Because of the limited number of these tests no definite conclusion can be shown although the fatigue life did not appear to be significantly affected by the reduction in temperature.

In random vibration fatigue tests it is necessary to truncate the applied loading spectrum to a prescribed value of root mean square stress above and below the root mean square value. The effect of the truncation level on fatigue endurance is dependent to a large extent on the root mean square value of the load spectrum concerned in relation to the fatigue limit strength of the structural element. Bending fatigue tests, about a zero mean load, on an aluminium-copper alloy have shown that truncation at a stress of  $\pm 2.5$  times the root mean square value results in lives greater than ten times those for specimens with load truncation at  $\pm 4.0$  times the root mean square value when the value of the root mean square stress is below the fatigue limit. The truncation levels for data presented are typical of the values found in normal acoustic environments, hence the data are directly applicable to structural elements subjects to acoustic loading.

The loading simulated for the skin-stiffener test specimens is that for modes in which skin-stiffener flexure predominate. Care should be taken when this Data Item is used for modes involving twisting of the stiffeners.

The reference stress for riveted-skin and rib-flange test specimens is the nominal root mean square stress (i.e. gross area measured r.m.s. stress between rivets) at the failure line. When using this Data Item to predict a life using a root mean square stress level obtained from Section 5 of Reference 1.7.9 it is recommended that the calculated value of root mean square stress at the rivet line should be used as the stress at the failure position. In practice the failure position is sufficiently close to the rivet line for this approximation to be within the range of accuracy of the simple theory used for stress prediction in Reference 1.7.9.

### 1.3 Plain Test Specimens

#### 1.3.1 Test specimens

The form of the cantilever test specimens is shown in Figure 1.1a. The material tested was 2024-T4.

#### 1.3.2 Method of testing

The test specimen was clamped at one end to a rigid mass and electromagnetic excitation was applied to the other end through a small steel plate attached to the specimen. The narrow band random excitation resulted in a Rayleigh distribution of peak loads in the test specimen at a resonant frequency of approximately 2000Hz. The stress level was monitored using a capacitive transducer located at the base of the test specimen. The transducer signal was integrated, with suitable time constant, by means of a true r.m.s. voltmeter which was first calibrated against a strain gauge placed at the failure position. Tests for failure were made using sinusoidal excitation, the criterion being the reduction of the resonance frequency to 98% of its original value.

In these tests the load was truncated at  $\pm 4$  times the root mean square stress.

#### 1.3.3 Test results

The results of plain cantilever fatigue tests are plotted on Figure 1.3. For these tests  $S_{\text{rms}}$  is the root mean square nominal bending stress in the skin at the failure line.

### 1.4 Integrally Machined Test Specimens

#### 1.4.1 Test specimens

The form of the machined stiffener and free-free beam test specimens are shown in Figure 1.1b and 1.1c. The material tested was VES(AL)504.

#### 1.4.2 Method of testing

The base of the machined stiffener test specimen rib was clamped to a moving coil vibrator being fed from a white noise generator. The signal from the noise generator was limited to a total bandwidth of  $1/3$  octave centred at the fundamental resonant frequency of the specimen. The resultant vibration of the specimen was in a mode corresponding to the fundamental natural mode varying randomly in amplitude. Failure was detected by the increase in damping and sharp reduction in resonant frequency accompanied by fluctuations in strain amplitude. In some cases the stress was monitored away from the failure line. For these cases the failure line stress was obtained using an experimentally determined factor.

The free-free beam was suspended on two elastic supports and excited at one end through a moving coil vibrator being fed from a white noise generator, as indicated in Figure 1.1c. The resultant vibration of the beam was in a mode corresponding to the fundamental natural bending mode.

In these tests the load was truncated between  $\pm 3.0$  and  $\pm 3.5$  times the root mean square stress.

#### 1.4.3 Test results

The results of machined stiffener and free-free beam tests are plotted on Figure 1.3. For these tests  $S_{rms}$  is the root mean square nominal stress at the failure position. A typical failure position for the machined stiffener is shown in Figure 1b. The failure position on the free-free beam was at the mid-position on the free edge of the stiffener web.

### 1.5 Riveted-Skin Test Specimens

#### 1.5.1 Test specimens

Form of the test specimens having single and double rows of skin attachment rivets is shown in Figures 1.2a and 1.2b.

For the specimens with a single row of skin attachment rivets four material types were tested D.T.D.710, D.T.D.746, D.T.D.5070 and 3.1364.5. Data for three types of rivet hole are presented, plain holes with mushroom-head

rivets, and  $100^\circ$  cut countersunk and  $100^\circ$  hot-pressure-dimpled holes with countersunk rivets. Data for two types of viscoelastic jointing compound are presented, type 1 to specification D.T.D.5605 (JC5A) and type 2 to specification D.T.D.4611 (Thiokol).

For the specimens with a double row of skin attachment rivets two material types were tested, D.T.D.710 and CMO01-1D. Data for both solid and blind countersunk rivets are presented with cut countersunk holes. A type 2 viscoelastic jointing compound to specification D.T.D. CMO21A (Viton) was used with solid countersunk rivets.

#### 1.5.2 Method of testing

The riveted-skin test specimens were tested in a similar manner to those used for the machined stiffener test specimens described in Section 1.4.2.

In these tests the load was generally truncated between  $\pm 3.0$  and  $\pm 3.5$  times the root mean square stress, although in a few tests the load truncation level was between  $\pm 4.4$  and  $\pm 4.6$  times the root mean square stress.

#### 1.5.3 Test results

The results of the riveted-skin fatigue tests are plotted in Figures 1.4 to 1.11 for the configurations shown in Table 1.1. For these tests  $S_{rms}$  is the root mean square nominal bending stress in the skin at the failure line. Figure 1.14 shows the position of skin cracks in the specimens with a single row of skin attachment rivets and Figure 1.15 shows the position of skin cracks in specimens with a double row of skin attachment rivets.

S-N data presented in Figure 1.7 indicates that there may be an effect of thickness on life; the test data for the 24 swg (0.558 mm) skin shows a lower life at any given stress level than that for thicker skins. The evidence of a thickness effect is not apparent in Figure 1.11 where different rivet holes are used. This suggests that the apparent thickness effect in Figure 1.7 results from stress concentrations at the rivet holes being more severe in the thinner skin for mushroom-head rivets in plain holes.

TABLE 1.1

FIGURE No.	SKIN MATERIAL	JOINTING COMPOUND	RIVET HOLE	RIVETS	RIVET MATERIAL SPECIFICATION
1.4	3.1364.5	none	plain	single row m/h	2.4360.1
1.5	CMO01-1D D.T.D.710	none none	c/s c/s	double row c/s double row c/s	BAS 7002* +
1.6	D.T.D.5070	type 1	plain	single row m/h	L 86
1.7	D.T.D.710 3.1364.5	type 2 type 2	plain plain	single row m/h single row m/h	L 86 2.4360.1
1.8	D.T.D.5070 D.T.D.710 D.T.D.746	type 1 type 1 type 1	c/s c/s c/s	single row c/s single row c/s single row c/s	L 86 L 69 L 69
1.9	D.T.D.710 CMO01-1D	type 2 type 2	c/s c/s	single row c/s double row c/s	L 86 BAS 7002*
1.10	3.1364.5	none	H.P.D.	single row c/s	2.4360.1
1.11	D.T.D.710	type 1	H.P.D.	single row c/s	L 86

m/h = mushroom-head  
c/s = countersunk  
H.P.D. = hot-pressure-dimpled

\* BAC specification  
+ monel and stainless steel

## 1.6 Rib-Flange Test Specimens

### 1.6.1 Test specimens

The form of the test specimens is shown in Figure 1.2c. Two material types were tested, D.T.D.710 and D.T.D.5070.

Data for two types of rivet hole are presented, plain holes with mushroom-head rivets, and 100° hot-pressure-dimpled holes with countersunk rivets. Data for two types of viscoelastic jointing compounds are presented, type 1 to specification D.T.D.5604 (JC5A) and type 2 to specification D.T.D.4611 (Thiokol).

### 1.6.2 Method of testing

The method of testing was as described in Section 1.4.2 with the test specimen skin clamped to the vibrator.

In these tests the load was truncated at  $\pm 3.2$  times the root mean square stress.

### 1.6.3 Test Results

The results of the rib-flange fatigue tests are plotted in Figure 1.12 and 1.13 for materials D.T.D.5070 and D.T.D.710 respectively. For these tests  $S_{rms}$  is the root mean square stress at the flange bend.

With few exceptions the failure originated in the flange bend. The exceptions were in a small number of specimens with type 1 viscoelastic jointing compound where failure originated at a rivet hole.

## 1.7 Derivation and References

### Derivation

1.7.1 Bayerdörfer, G.  
Carl, R.

Unpublished work by Dornier AG.

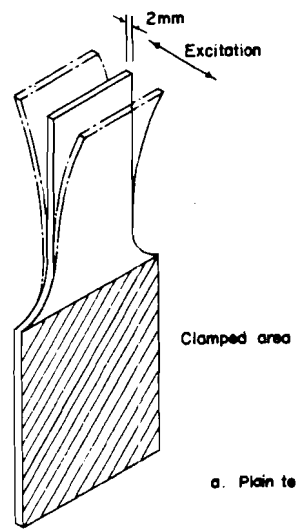
1.7.2 Townsend, N.A.  
Corke, D.M.

The fatigue strength between  $10^5$  and  $10^{10}$  cycles to failure of light alloy skin-rib joints under fully reversed bending loads.  
Part 2 - Random amplitude excitation.  
Hawker Siddeley Aviation Ltd. Stress Office  
Report 54. Work under Ministry of Aviation  
contract KS/1/0115/C.B.43(a)2, May 1963.

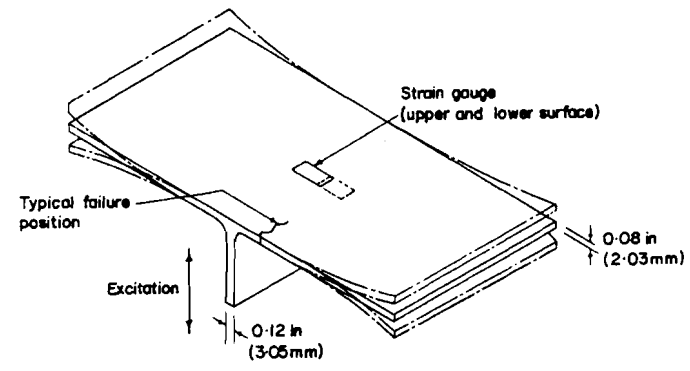
- 1.7.3 Cummins, R.J.  
Eaton, D.C.G. Unpublished work by British Aircraft Corporation, May 1969.
- 1.7.4 Townsend, N.A. Fully reversed bending r.m.s. S-N curves for light alloy skin rib joints between  $10^5$  and  $10^9$  cycles to failure. Part 1 - unreinforced skins. Hawker Siddeley Aviation Ltd. Stress Office Report AR 10. Work under Ministry of Technology contract KS/1/0401/C.B.43(a)2, June 1970.
- 1.7.5 Artusio, G.  
et al. Unpublished work by Fiat, January 1971.
- 1.7.6 Cummins, R.J.  
Eaton, D.C.G. Unpublished work by British Aircraft Corporation, January 1971.
- 1.7.7 Bayerdörfer, G. Experimental investigation to establish acoustic fatigue design charts. J. Sound Vib., Vol.17, No.1, pp.55-62, July 1971.

#### References

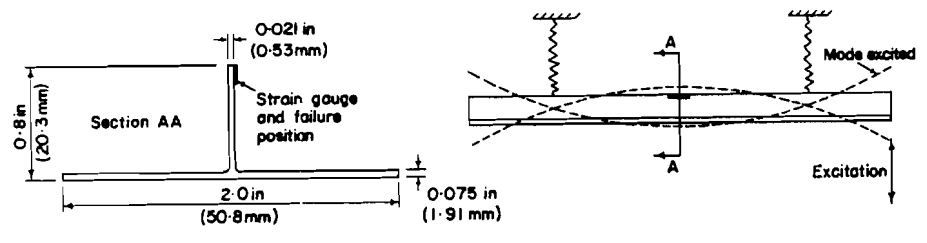
- 1.7.8 Kirkby, W.T. A review of the work in the United Kingdom on the fatigue of aircraft structures during the period May 1969-May 1971. RAE tech. Rep. 71157, August 1971.
- 1.7.9 Thomson, A.G.R. Acoustic fatigue design data. AGARD-AG-162-Part 1, May 1972.



a. Plain test specimen



b. Machined stiffener test specimen



c. Free-free beam

FIGURE 1.1.

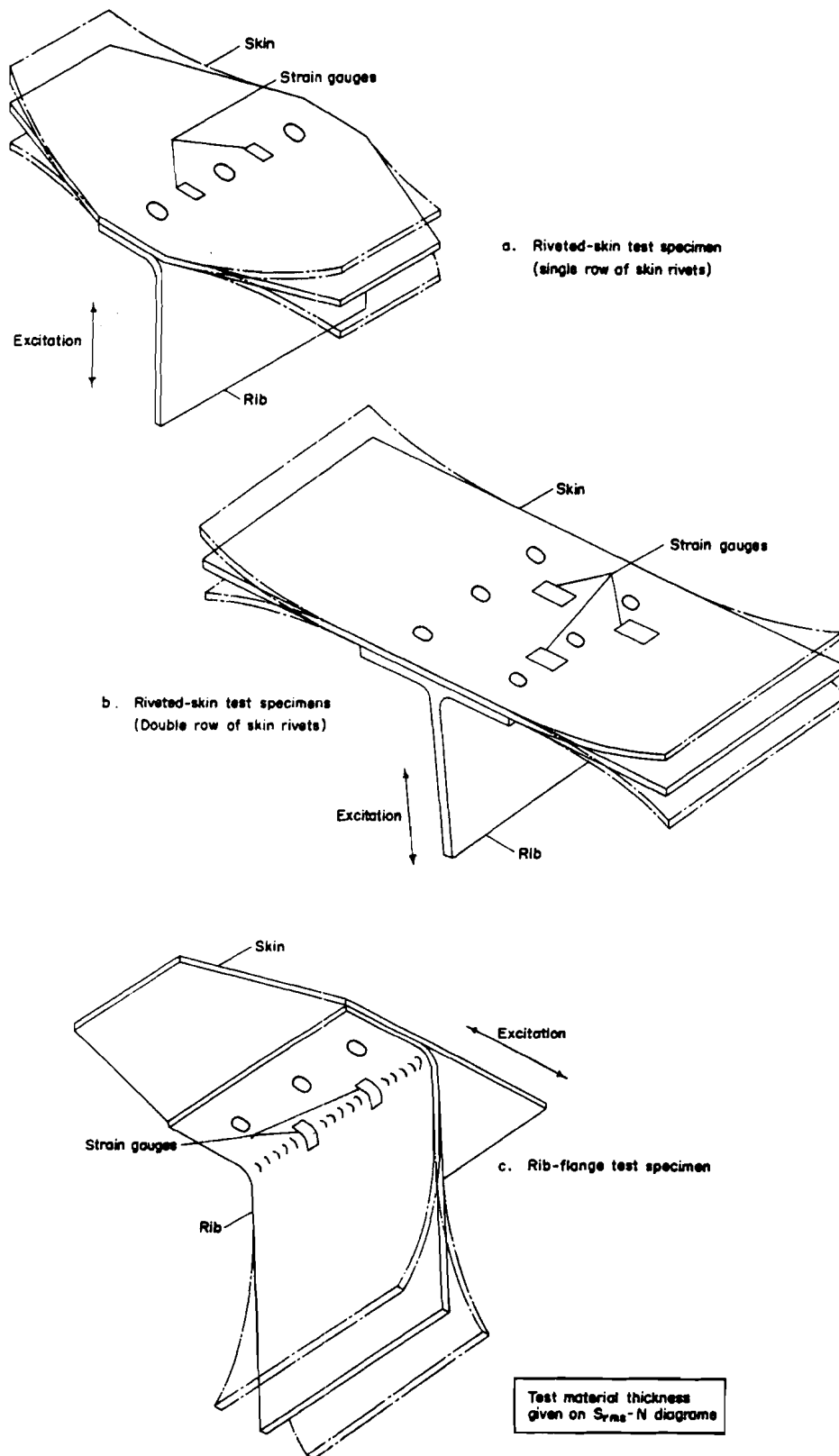


FIGURE 1.2.

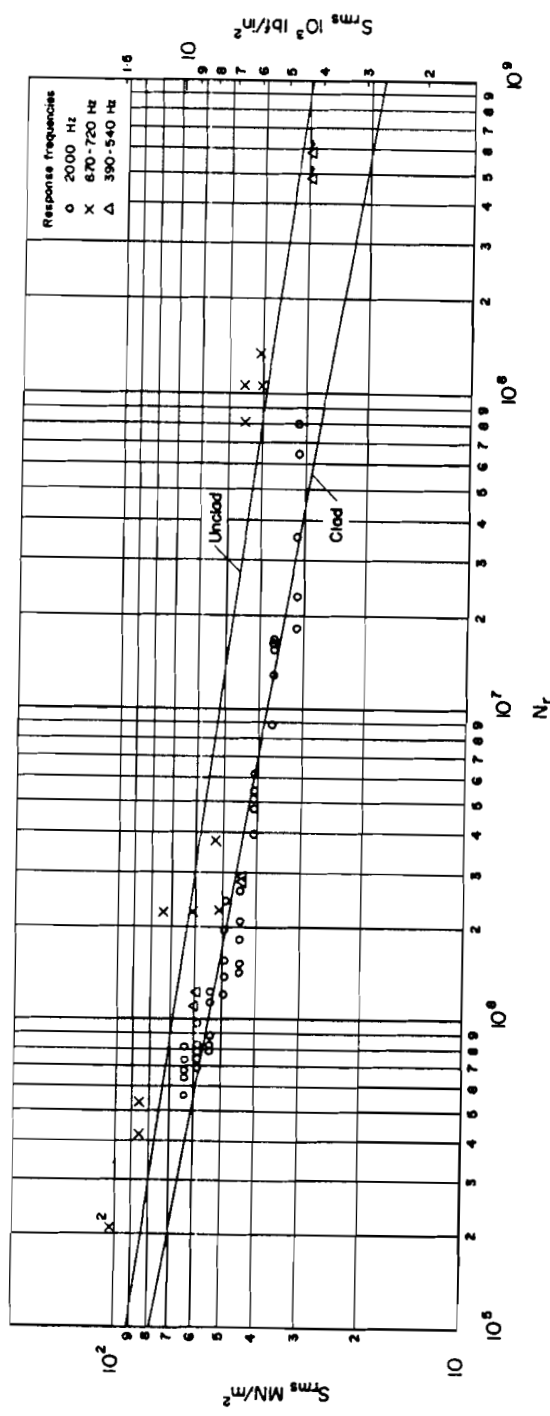


FIGURE I.3. S-N DATA FOR PLAIN AND MACHINED STIFFENER SPECIMENS

Code	Specimen type	Material	Type of failure	Failure Log Fig. No.
○	Plain specimen	2024-T4 (Clad)	Crack near clamped position	—
X	Machined stiffener	VES(AL)504 (Unclad)	Machined skin crack	1b
△	Machined free-free beam	VES(AL)504 (Unclad)	Beam vertical flange crack	1c

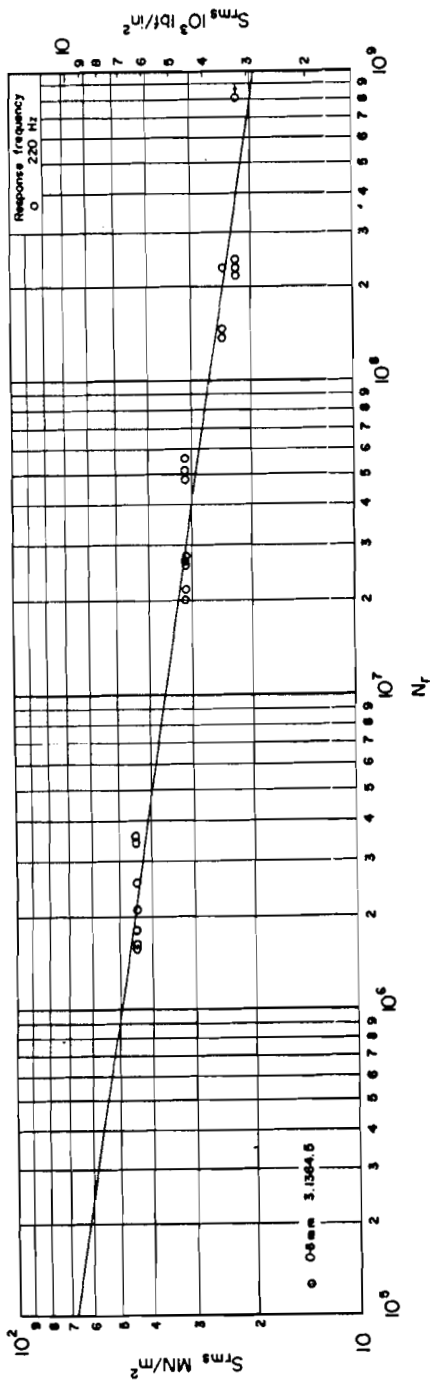


FIGURE 1.4. S-N DATA FOR RIVETED SKIN - PLAIN HOLES - NO JOINTING COMPOUND

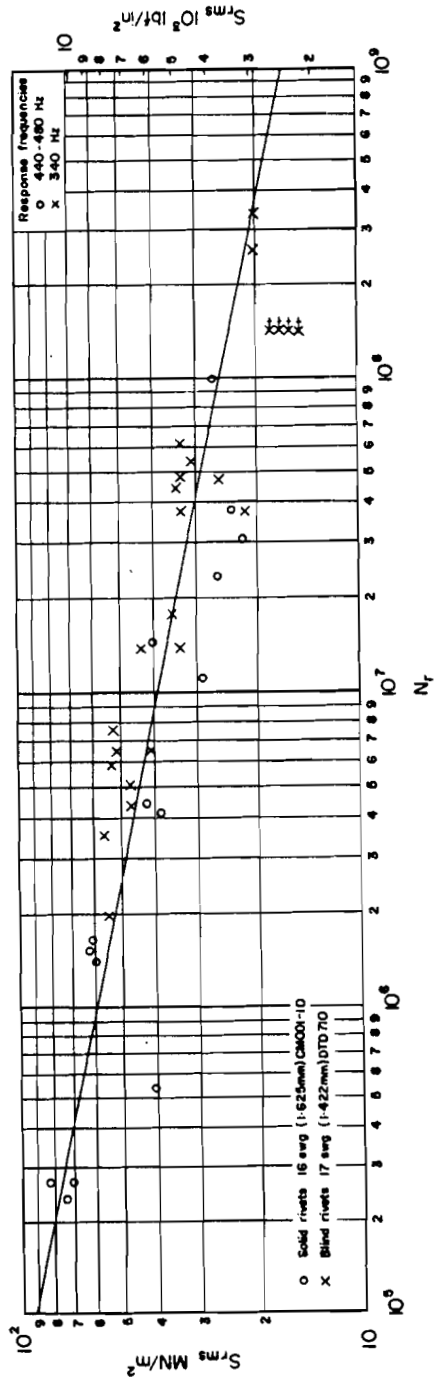


FIGURE 1.5. S-N DATA FOR RIVETED SKIN - CUT COUNTERSUNK HOLES - NO JOINTING COMPOUND

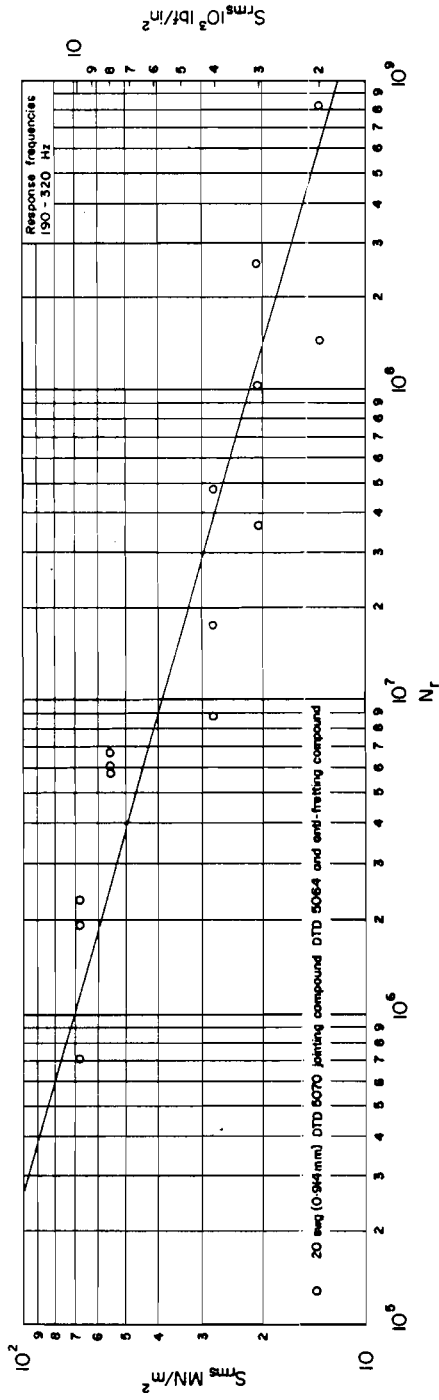


FIGURE 1.6. S-N DATA FOR RIVETED SKIN - PLAIN HOLES - TYPE 1 VISCOELASTIC JOINTING COMPOUND

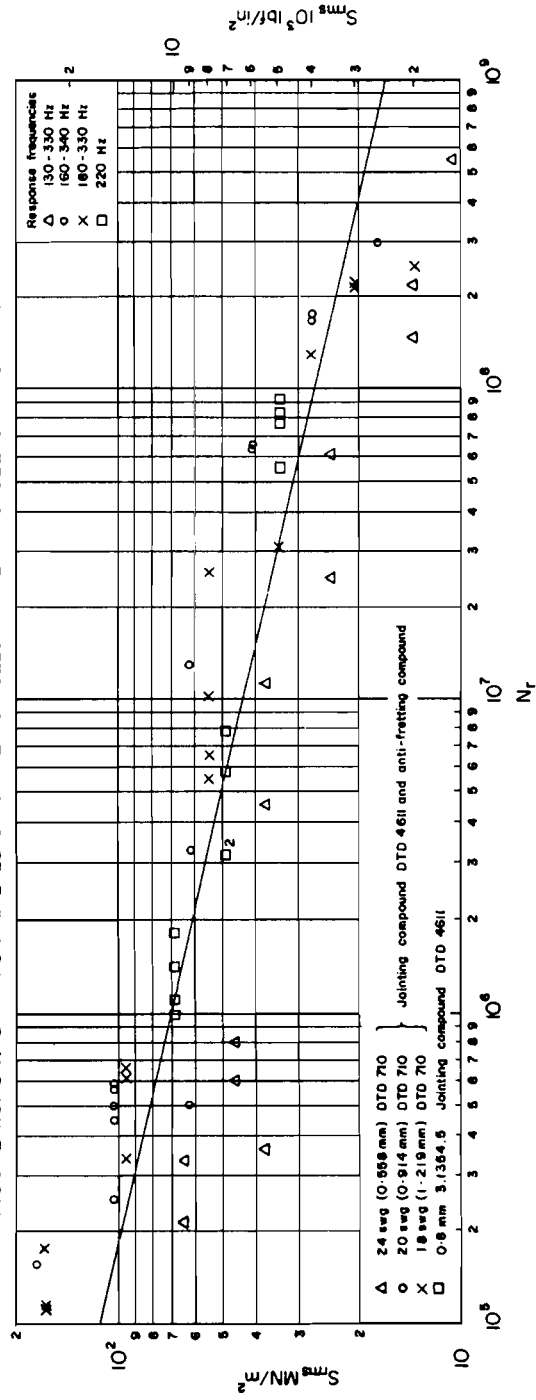


FIGURE 1.7. S-N DATA FOR RIVETED SKIN - PLAIN HOLES - TYPE 2 VISCOELASTIC JOINTING COMPOUND

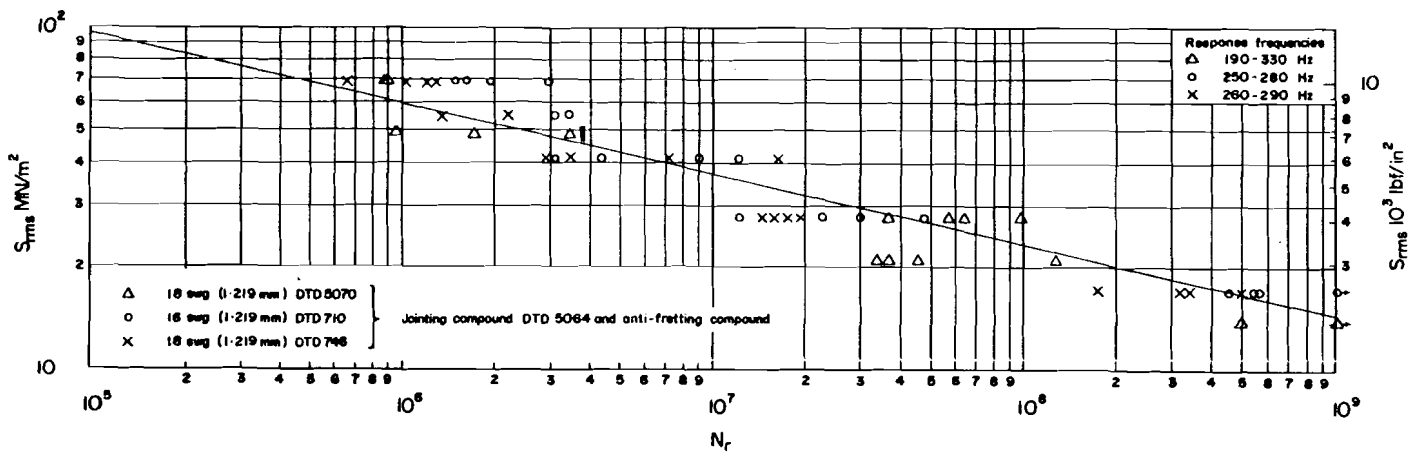


FIGURE 1.8. S-N DATA FOR RIVETED SKIN - CUT COUNTERSUNK HOLES - TYPE 1 VISCOELASTIC JOINTING COMPOUND

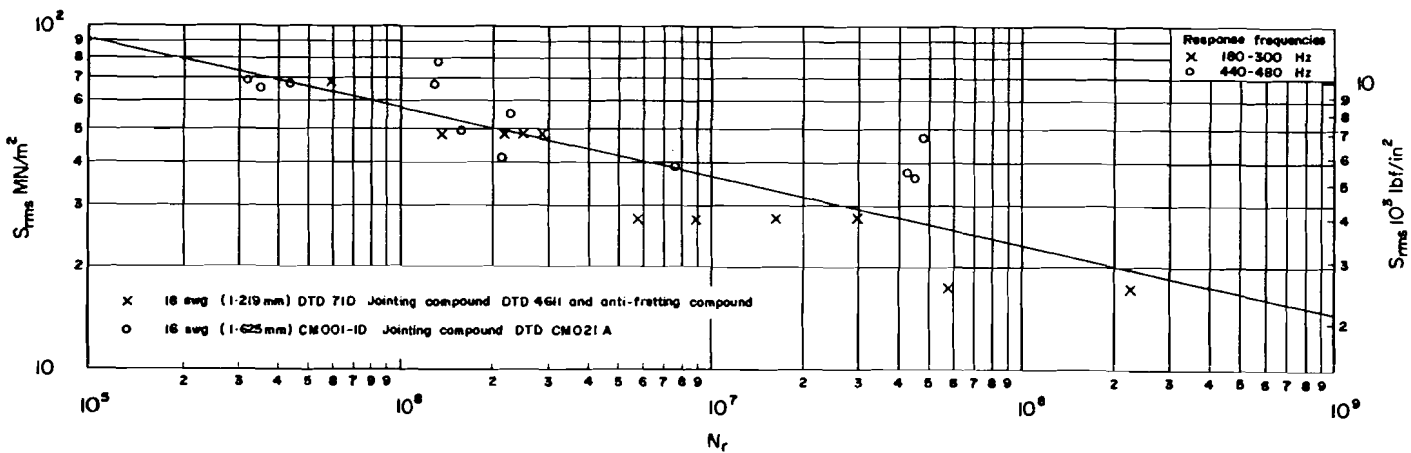


FIGURE 1.9. S-N DATA FOR RIVETED SKIN - CUT COUNTERSUNK HOLES - TYPE 2 VISCOELASTIC JOINTING COMPOUND

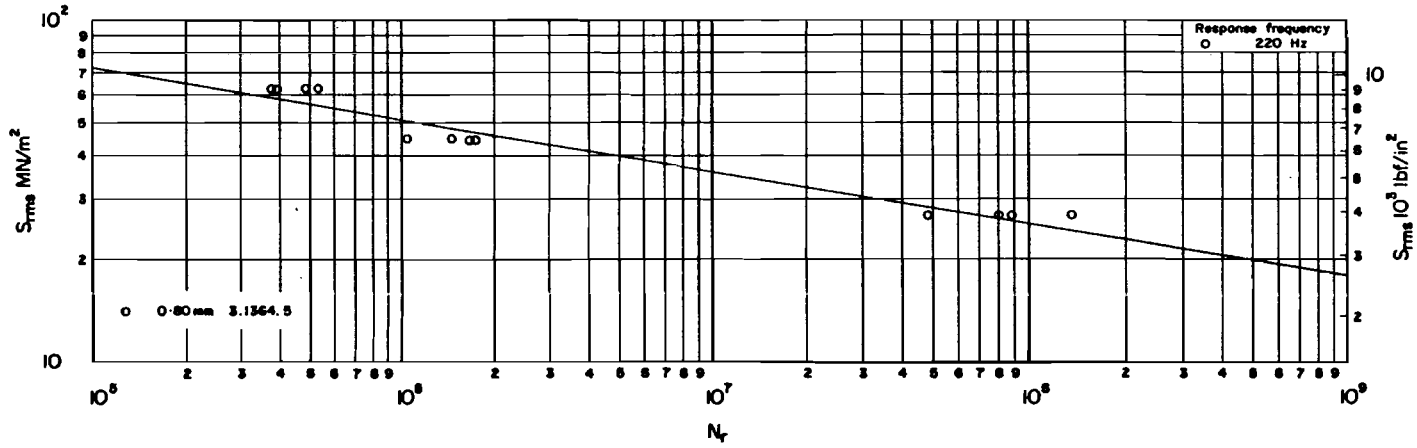


FIGURE I. IO. S-N DATA FOR RIVETED SKIN - HOT PRESSURE DIMPLED HOLES - NO JOINTING COMPOUND

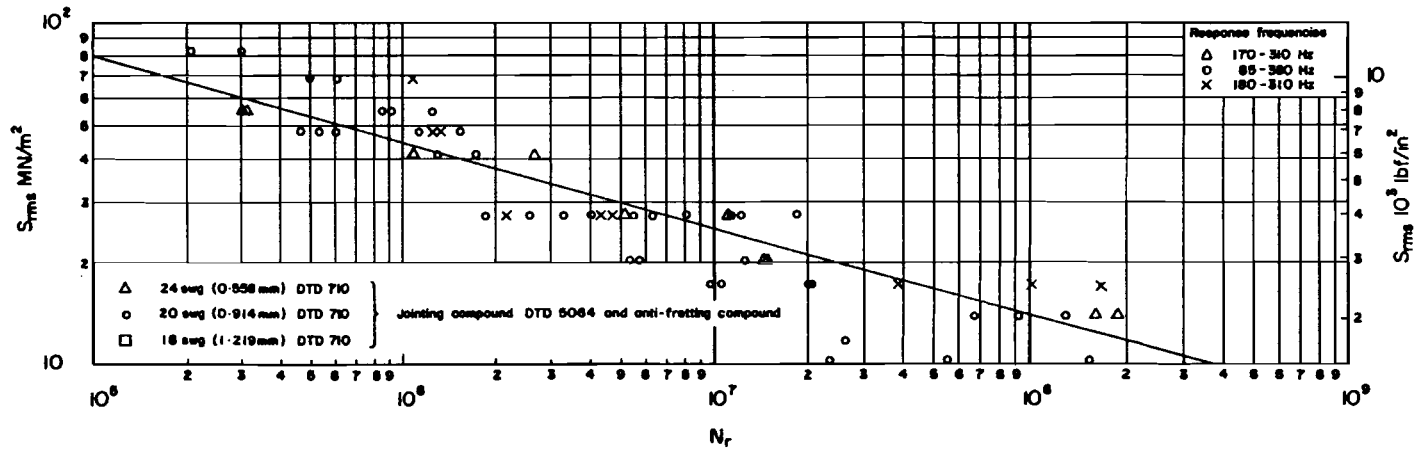


FIGURE I. II. S-N DATA FOR RIVETED SKIN - HOT PRESSURE DIMPLED HOLES - TYPE I VISCOELASTIC JOINTING COMPOUND

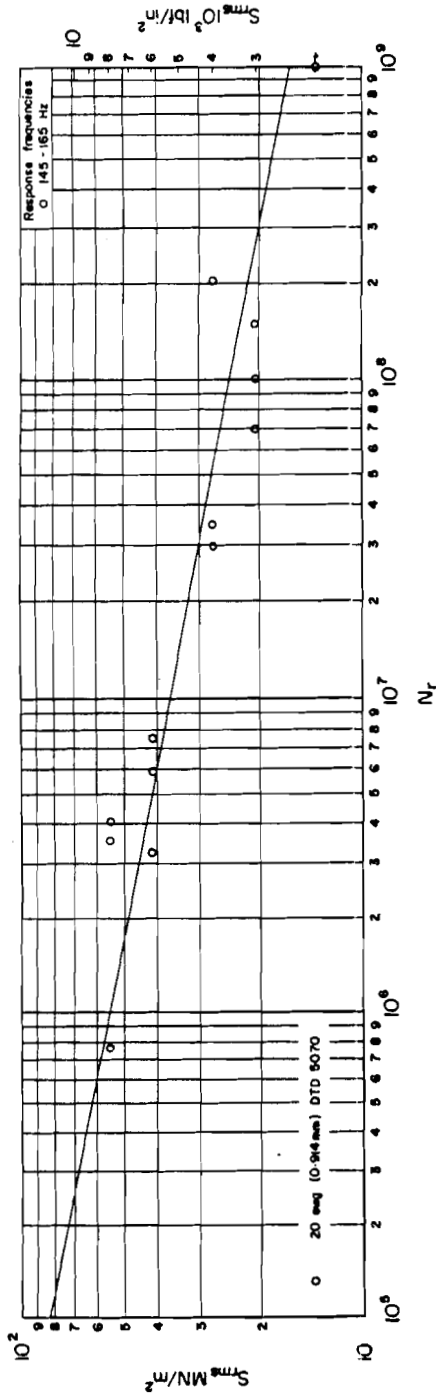


FIGURE 1.12. S-N DATA FOR RIB FLANGE

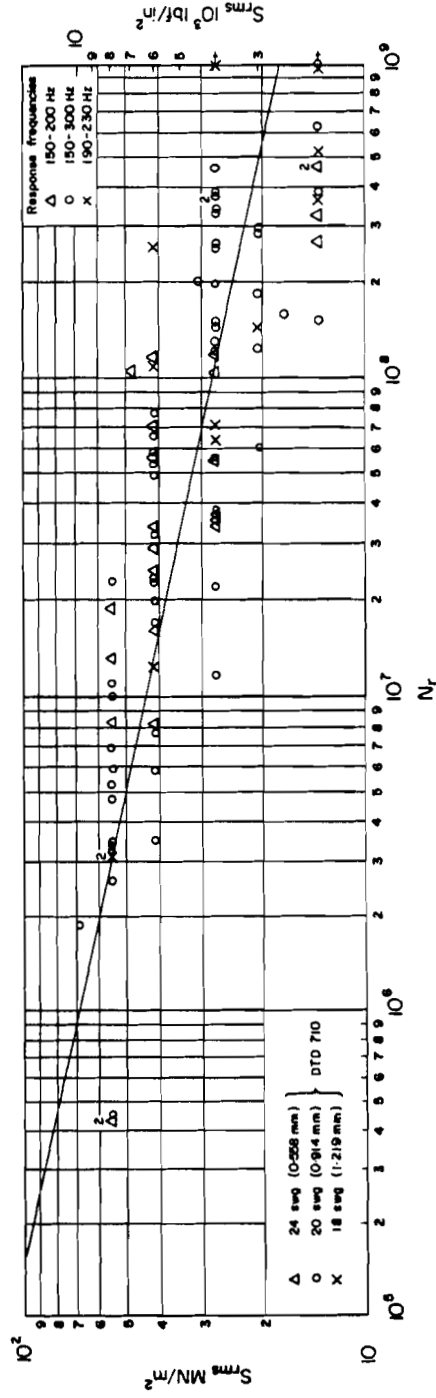


FIGURE 1.13. S-N DATA FOR RIB FLANGE

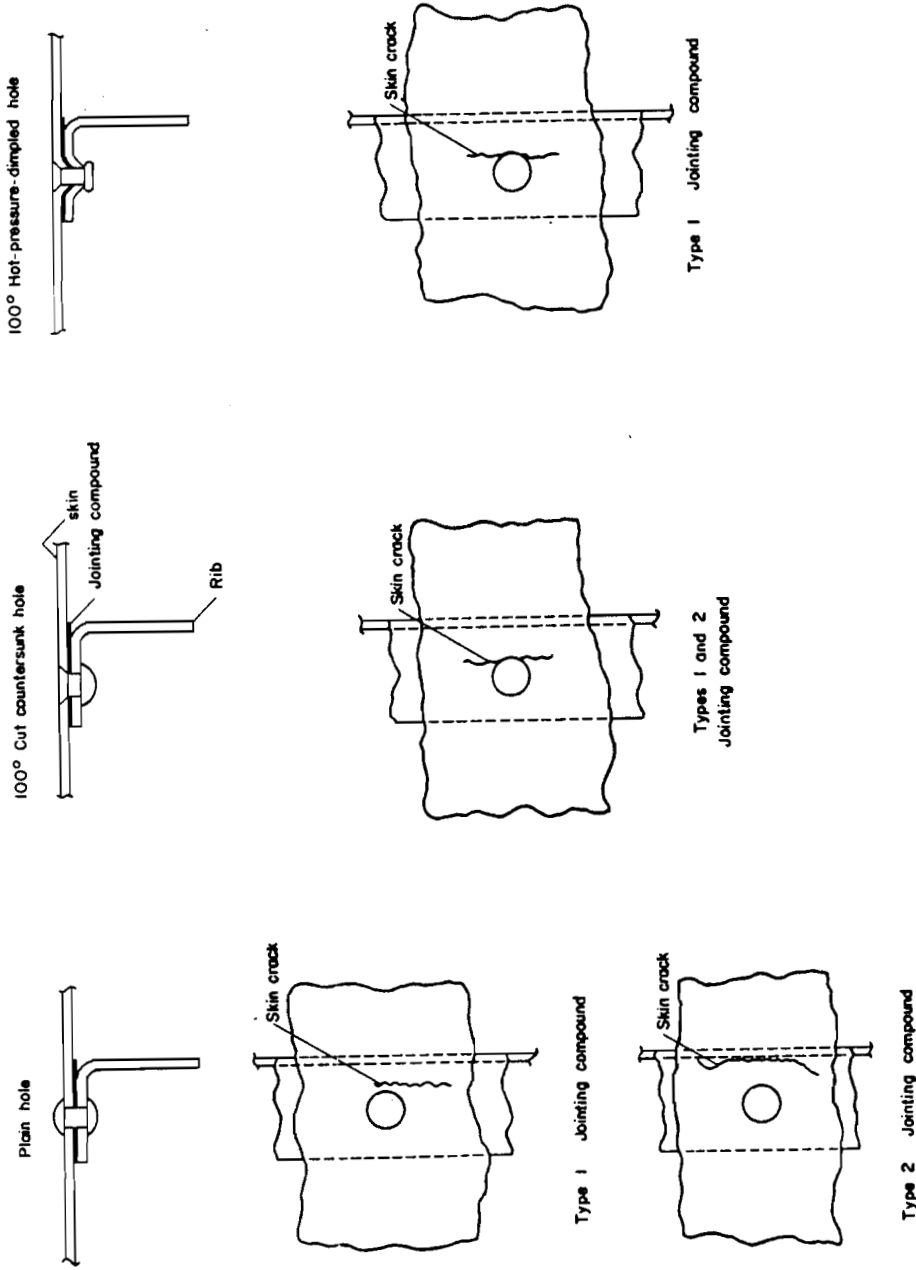


FIGURE 1.14. TYPICAL FAILURES IN RIVETED-SKIN TEST SPECIMENS

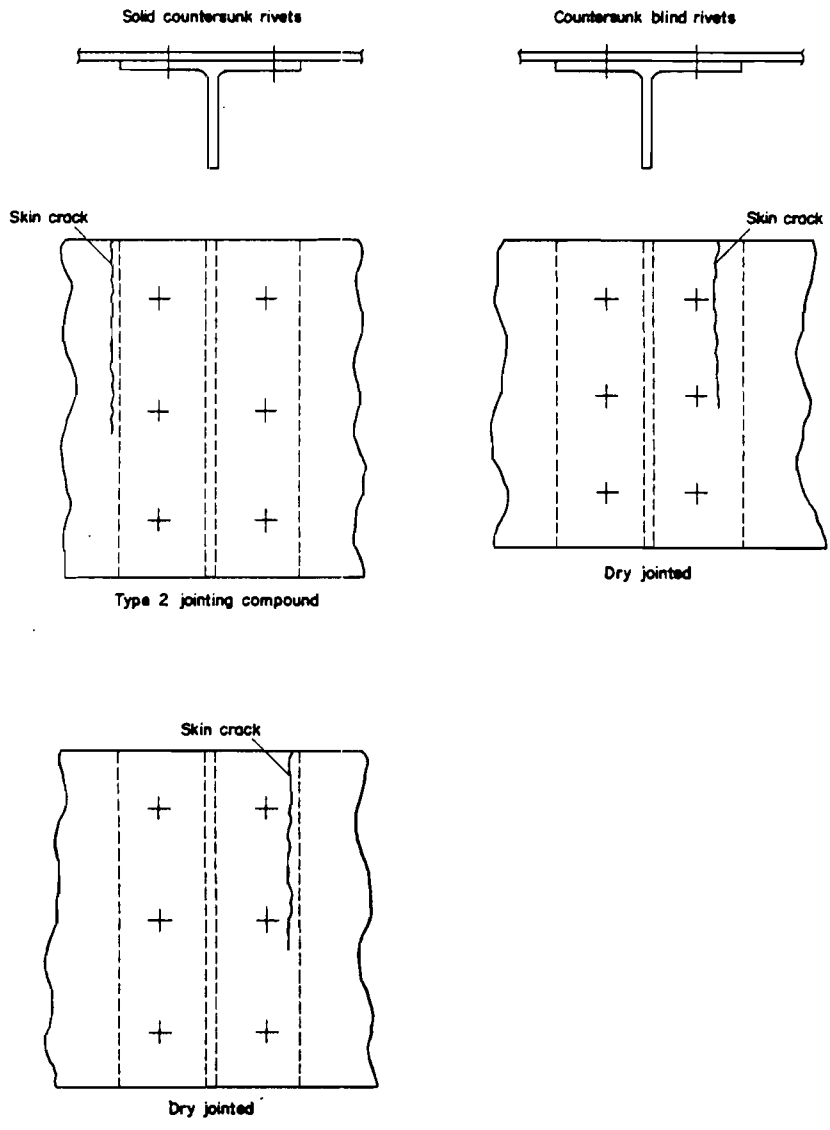


FIGURE I.15. FAILURES IN RIVETED-SKIN TEST SPECIMENS (DOUBLE ROW SKIN RIVETS)

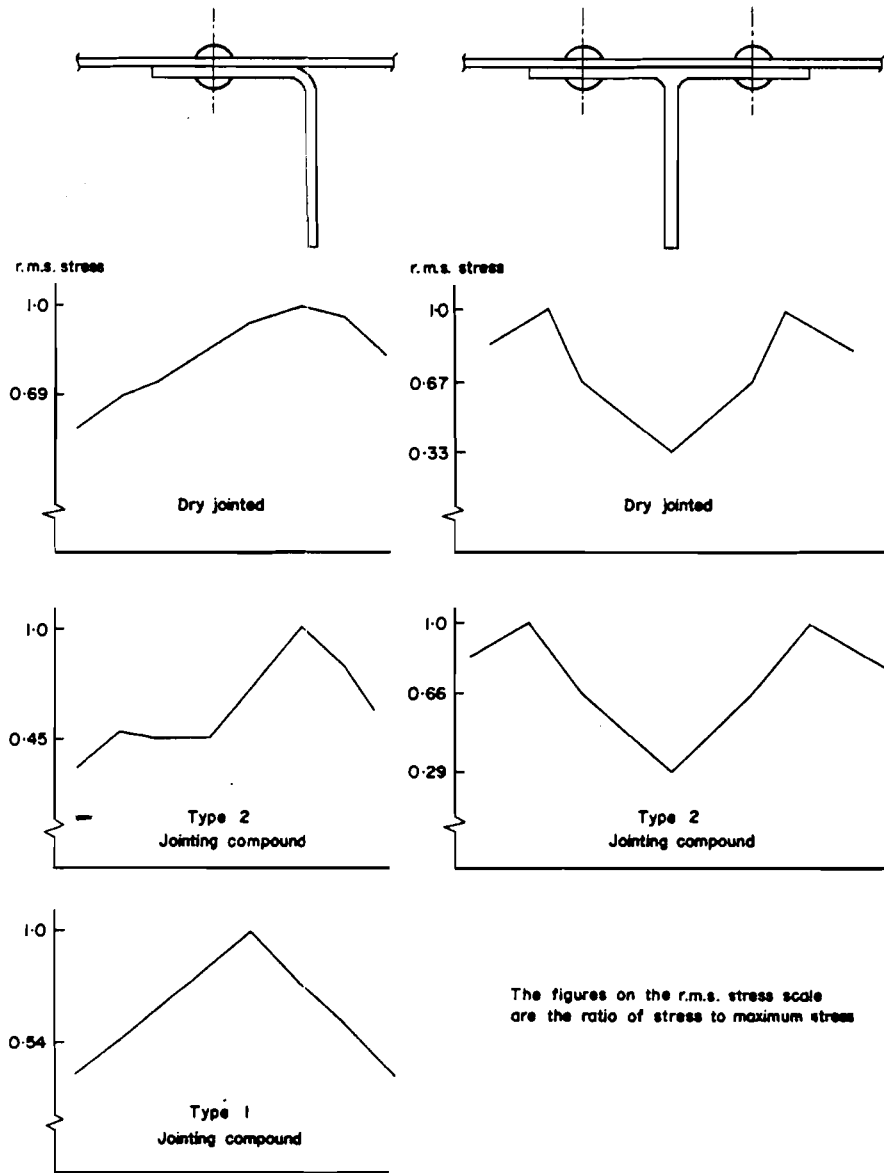


FIGURE 1.16. STRESS DISTRIBUTIONS OVER RIVETED-SKIN TEST SPECIMENS

APPENDIX 1A1A. Materials1A.1 General Description

2024-T4	Aluminium-copper-magnesium-manganese alloy sheet clad with aluminium. Solution heat treated and naturally aged.
3.1364.5	Aluminium-copper-magnesium-manganese alloy sheet clad with aluminium. Solution heat treated followed by strain hardening.
D.T.D. 710	Aluminium-copper-magnesium-silicon-manganese alloy sheet clad with aluminium. Solution heat treated and naturally aged.
D.T.D. 746	Aluminium-copper-magnesium-silicon-manganese alloy sheet clad with aluminium. Solution heat treated and artificially aged.
D.T.D. 5070	Aluminium-copper-magnesium-nickel-iron alloy sheet clad with aluminium-zinc alloy. Solution heat treated and artificially aged.
CM001-1D (BAC designation)	Aluminium-copper-magnesium-silicon-nickel-iron alloy sheet clad with aluminium-zinc alloy. Solution heat treated and artificially aged.
VES(AL)504 (BAC designation)	Aluminium-copper-magnesium-nickel-iron alloy plate. Solution heat treated and artificially aged.

1A.2 Material Chemical Composition

In Table 1A.1 the chemical compositions of the core material and cladding are listed for materials considered in this Section. The values given are the limits of each alloying element as a percentage by weight of the total.

1A.3 Equivalent Materials and Tensile Properties

In Table 1A.2 the tensile strength of the materials for which data are presented is given. The strength values quoted are applicable to the material thicknesses considered in this Section.

For the materials for which data are presented the equivalent, or nearest equivalent, Aluminium Association alloy is given in Table 1A.2. The U.S. designation of the equivalent heat treatment condition is also listed. Other national standard designations may be found in the latest editions of References 1A.4.1 and 1A.4.2.

1A.4 References

1A.4.1	-	Conversion charts, data sheets and equivalence lists for American aircraft materials. NATO document AC/82-D/4.
1A.4.2	-	Aluminium standards and data. Aluminium Association, New York.

TABLE 1A.1

MATERIAL ELEMENT		2024 3.1364		D.T.D. 710 D.T.D. 746		D.T.D. 5070 CM001-1D		VES(AL) 504 PLATE
		CORE	CLADDING	CORE	CLADDING	CORE	CLADDING	
	Cu	3.8 to 4.9	0.1 max.	3.8 to 4.8	0.02 max.	1.8 to 2.7	—	As core of D.T.D. 5070
	Mg	1.2 to 1.8	—	0.55 to 0.85	—	1.2 to 1.8	—	
	Mn	0.3 to 0.9	0.05 max.	0.4 to 1.2	—	0.2 max.	—	
	Fe	0.5 max.	Fe+Si 0.7 max.	1.0 max.	0.2 max.	0.9 to 1.4	—	
	Si	0.5 max.		0.6 to 0.9	0.15 max.	—	—	
	Zn	0.25 max.	—	0.2 max.	0.03 max.	0.1 max.	0.8 to 1.2	
	Ni	—	—	0.2 max.	—	0.8 to 1.4	—	
	Pb	—	—	0.05 max.	—	0.05 max.	—	
	Sn	—	—	0.05 max.	—	0.05 max.	—	
	Cr	0.1 max.	—	Cr+Ti 0.3 max.	—	—	—	
	Ti	* *	* *		—	0.2 max.	—	
others	Each	0.05 max.	0.05 max.	—	—	—	—	
	Total	0.15 max.	0.15 max.	—	—	—	—	
	Al	REM	REM	REM	99.7 min.	REM	REM	

REM = REMAINDER

\* for 2024 0.°/o and 3.1364 Ti + Zr 0.2°/o max.

+ for D.T.D. 5070 0.25°/o max. and for

CM001-D 0.15 to 0.25°/o

TABLE 1A.2

Material Tested	AA Alloy	Heat Treatment Condition	Tensile Strength MN/m <sup>2</sup>
2024-T4	2024	T4	457
3.1364.5	2024	T3	402
D.T.D. 710	2014 or 2024	T4	386
D.T.D. 746	2014 or 2024	T6	417 <sup>*</sup>
D.T.D. 5070	2618	T6	390
CM001-1	2618	T6	394
VES(AL) 504	2618	T6	402

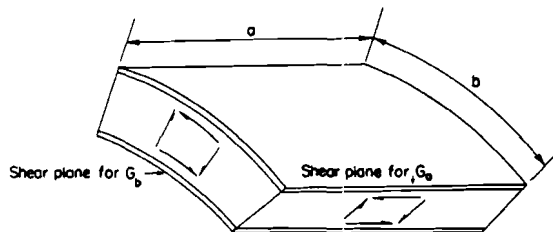
\* For thickness 20 swg to 24 swg (0.914 mm to 0.558 mm).  
For thickness 17 swg to 19 swg (1.422 mm to 1.016 mm) 425 MN/m<sup>2</sup>.

## Section 2

NATURAL FREQUENCIES OF FLAT OR SINGLY-CURVED SANDWICH PANELS  
WITH CORES OF ZERO FLEXURAL STIFFNESS

## 2.1 Notation

$a$	longer dimension of flat panel, or length of curved panel straight edge	m	in
$b$	shorter dimension of flat panel or arc length of curved panel	m	in
$C_1, C_2, C_3$	non-dimensional parameters (see Derivation)		
$E$	Young's modulus of face-plate material	$N/m^2$	$lbf/in^2$
$F$	non-dimensional parameter (see Derivation)		
$f_c$	natural frequency of curved panel	Hz	c/s
$f_f$	natural frequency of flat panel	Hz	c/s
$f_u$	natural frequency of uniform flat plate of thickness equal to distance between midplanes of face plates and having density and Young's modulus equal to those of the face plates	Hz	c/s
$G$	shear modulus of honeycomb core material	$N/m^2$	$lbf/in^2$
$G_a, G_b$	transverse shear moduli of core in planes defined in sketch below	$N/m^2$	$lbf/in^2$



$G_c$	effective shear modulus of core	$N/m^2$	$lbf/in^2$
$G_x, G_y$	transverse shear moduli of core in planes defined in sketch on page 20	$N/m^2$	$lbf/in^2$
$h$	core thickness	m	in
$K_1, K_2$	non-dimensional parameters (see Derivation)		
$l$	length of honeycomb cell wall	m	in
$m$	number of half-waves parallel to side of length $a$		
$n$	number of half-waves parallel to side of length $b$		
$R$	radius of curvature of panel	m	in
$t$	face-plate thickness	m	in
$t_c$	thickness of honeycomb core material	m	in
$\rho_c$	core density	$kg/m^3$	$lb/in^3$
$\rho_f$	face-plate density	$kg/m^3$	$lb/in^3$
$\sigma$	Poisson's ratio of face-plate material		

Both SI and British units are quoted but any coherent system of units may be used.

2.2 Notes

This Section gives a method of calculating the natural frequencies of initially unstressed flat or curved rectangular panels of sandwich construction with identical face plates. The core is assumed to have zero flexural stiffness and to be isotropic, but a moderate degree of orthotropy i.e.  $1/3 < G_a/G_b < 3$  can be taken into account. The data have been derived for application to honeycomb sandwich panels, but may be used for other types of sandwich panel having cores of negligible flexural stiffness provided that their properties comply with the assumptions stated later in these notes.

The natural frequency of the sandwich panel is obtained by factoring the natural frequency,  $f_u$  of a solid flat plate of thickness equal to the distance between the mid-planes of the face plates,  $h+t$ , according to the following expressions.

For a flat panel:

$$f_f = f_u C_1 C_2$$

For a curved panel:

$$f_c = f_f \left\{ 1 + \left( \frac{b^2}{n^2 R(h+t)} \right)^2 \frac{C_3}{C_2^2} \right\}^{1/2}$$

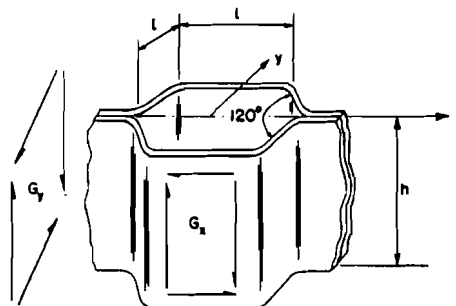
The values of  $f_u$ ,  $C_1$ ,  $C_2$ ,  $C_3$  and  $f_c$  are obtained as shown in the following Table.

Parameter:	obtained from:	as a function of:
$f_u$	Reference 2.3.2, 2.3.5 or 2.3.6	$\frac{h}{b^2}$ , $\frac{a}{b}$ , $m$ , $n$ , edge conditions
$C_1$	Figure 2.1	$\frac{\rho_c h}{\rho_f t}$
$G_c/G_a$	Figure 2.2	$\frac{mb}{an}$ , $\frac{G_b}{G_a}$
$C_2$	Figure 2.3	$\frac{E}{G_c} \frac{t}{h} \frac{(h+t)^2 m^2}{a^2}$ , $\frac{mb}{an}$
$C_3$	Figure 2.4	$\frac{mb}{an}$
$f_c/f_f$	Figure 2.5	$C_2$ , $C_3$ , $\frac{b^2}{n^2 R(h+t)}$

The shear moduli of the core,  $G_a$  and  $G_b$ , can be obtained from manufacturers' data or test, or they can be calculated for honeycomb cores. A suitable test method is described in Reference 2.3.3 and a calculation method for hexagonal honeycomb cores is given in Reference 2.3.4. For the case of deep hexagonal honeycomb cores with  $h/l > 2$ , and included angle of  $120^\circ$ ,

$$G_y = 0.577 \frac{t_c}{l} G$$

and  $G_x = 1.5 G_y$ .



Shear moduli of different samples of core may be expected to vary by up to about 25%, but the effect on natural frequency is significant only when  $C_2$  is much less than unity.

The data are based on an exact solution of the simplified differential equation of motion of an idealised slightly-curved panel described in Derivation 2.3.1.

It is assumed that the orthotropic core carries no in-plane loading, but carries all the transverse shear. The method of accounting for orthotropy has been simplified to allow graphical presentation, but the errors arising from this simplification do not exceed 1 per cent over the ranges of variables covered by the Figures.

The panel is assumed to be simply-supported at all edges, but it is suggested that provided  $C_2$  is close to unity the fundamental natural frequency for panels with fixed edges can be found approximately by taking  $f_u$  corresponding to fixed-edge conditions for a uniform plate.

The frequencies of the higher modes of curved panels are obtained approximately by assuming that the frequencies are the same as for a simply-supported panel having dimensions of one half wavelength in each direction, i.e. by substituting  $a/m$  and  $b/n$  for  $a$  and  $b$ . Frequencies calculated this way compare well with the few experimental results that are available for modes up to (3,1) or (1,3).

It is assumed that the half-wavelengths are large compared with the cell-size of honeycomb core, and that there is no strain in the through-thickness (radial) direction. These assumptions are not expected to lead to serious error for conventional sandwich panels covered by the ranges of variables given in Figures 2.1 to 2.4, but any extrapolation outside these ranges should be treated with caution.

Figures 2.3 and 2.4 are drawn for a value of  $\sigma = 0.3$ .

A computer program to calculate both natural frequencies and stress response, based in part on this Section, is given in Section 3 of this AGARDograph.

## 2.3 Derivation and References

### Derivation

The frequency expressions are:

$$f_f = f_u C_1 C_2,$$

$$\text{and } f_g = f_f \left\{ 1 + \left( \frac{b^2}{n^2 R(h+t)} \right)^2 \frac{C_3}{C_2^2} \right\}^{1/2}$$

where  $f_u$  is obtained from Reference 2.3.2, 2.3.5 or 2.3.6 and

$$C_1 = \left\{ \frac{6}{\left(2 + \frac{\rho_g h}{\rho_f t}\right)} \right\}^{1/2},$$

$$C_2 = \left[ \left( \frac{E}{G_c} \right) \left( \frac{t}{h} \right) \frac{(h+t)^2 m^2}{a^2} \frac{\pi^2}{2(1-\sigma^2)} \left\{ 1 + \left( \frac{an}{mb} \right)^2 \right\} + 1 \right]^{-1/2}$$

$$\text{and } C_3 = \frac{4}{\pi^4} \frac{\left\{ 1 - \left( \frac{an}{mb} K_2 + \sigma K_1 \right) \right\}}{\left\{ 1 + \frac{m^2 b^2}{a^2 n^2} \right\}^2},$$

$$\text{where } K_1 = \frac{2}{F} \left[ \frac{a^2 n^2}{m^2 b^2} (1+\sigma) - \sigma \left\{ 2 \frac{a^2 n^2}{m^2 b^2} + 1 - \sigma \right\} \right],$$

$$K_2 = \frac{2}{F} \left[ (1+\sigma) \sigma - \left\{ 2 + \frac{a^2 n^2}{m^2 b^2} (1-\sigma) \right\} \right],$$

$$F = \frac{a^2 n^2}{m^2 b^2} (1+\sigma)^2 - \left[ 2 \frac{a^2 n^2}{m^2 b^2} + 1 - \sigma \right] \left[ 2 + \frac{a^2 n^2}{m^2 b^2} (1-\sigma) \right],$$

and

$$G_c = \frac{G_a \left( 1 + \frac{a^2 n^2}{m^2 b^2} \right)}{\left( 1 + \frac{a^2 n^2 G_a}{m^2 b^2 G_b} \right)}$$

- 2.3.1 Jacobson, M.J. Stress and deflection of honeycomb panels loaded by spatially uniform white noise. AIAA Journal, Vol.6, No.8, August 1968.

#### References

- 2.3.2 - Natural frequencies of uniform flat plates. Engineering Sciences Data Item No.66019, 1966.
- 2.3.3 - Experimental determination of the shear and flexural stiffnesses of a sandwich panel. Engineering Sciences Data Item No.66025, 1966.
- 2.3.4 - Modulus of rigidity of sandwich panels with hexagonal cell cores. Engineering Sciences Data Item No.67022, 1967.
- 2.3.5 Thomson, A.G.R. Natural frequencies of rectangular singly-curved plates. Acoustic fatigue design data, Part 1, Section 4. AGARDograph 162, Part 1, May 1972.
- 2.3.6 - Natural frequencies of rectangular singly-curved plates. Engineering Sciences Data Item No.72004, 1972.

#### 2.4 Example

It is required to estimate the natural frequency in the mode with one half wavelength in each direction of a singly-curved honeycomb sandwich panel with simply-supported edges having the following dimensions and material properties:

$$\begin{aligned} a &= 450 \text{ mm}, & b &= 300 \text{ mm}, & t &= 0.5 \text{ mm}, & h &= 10 \text{ mm}, & R &= 1600 \text{ mm}, \\ E &= 70\,400 \text{ MN/m}^2, & G_a &= 141 \text{ MN/m}^2, & G_b &= 212 \text{ MN/m}^2, & \rho_f &= 2660 \text{ kg/m}^3, \\ & & \rho_c &= 64.0 \text{ kg/m}^3, & \sigma &= 0.3. \end{aligned}$$

Hence  $\frac{a}{b} = 1.5$

and from Reference 2.3.5

$$K_{m,n} = 3.47 \times 10^3 \text{ m/s}, \quad V = 1.013$$

and  $f_u = 3.47 \times 10^3 \times 1.013 \times \frac{0.0105}{(0.300)^2}$

$$= 410 \text{ Hz.}$$

Now  $\frac{\rho_c h}{\rho_f t} = \frac{64.0 \times 10 \times 10^{-3}}{2660 \times 0.5 \times 10^{-3}} = 0.481$ .

Therefore from Figure 2.1,

$$C_1 = 1.555.$$

From Figure 2.2, for  $\frac{mb}{an} = 0.667$  and  $\frac{G_b}{G_a} = 1.5$ ,  $\frac{G_c}{G_a} = 1.29$ .

Hence  $G_c = 1.29 \times 141 = 182 \text{ MN/m}^2$ .

From Figure 2.3, for

$$\left( \frac{E}{G_c} \right) \left( \frac{t}{h} \right) \frac{(h+t)^2 m^2}{a^2} = \frac{70\,400}{182} \times \frac{0.5}{10} \times \frac{10.5^2 \times 1^2}{450^2} = 10.5 \times 10^{-3},$$

and for  $\frac{mb}{an} = 0.667$ , by interpolation,

$$C_2 = 0.915 .$$

From Figure 2.4, for  $\frac{mb}{an} = 0.667$ , by interpolation,

$$C_3 = 0.0082 .$$

Hence  $f_f = f_u C_1 C_2 = 410 \times 1.555 \times 0.915 = 583 \text{ Hz}.$

Now  $\frac{b^2}{n^2 R(h+t)} = \frac{300^2}{1^2 \times 1600 \times 10.5} = 5.36$

and from Figure 2.5, the point  $q$  on the pivot line is obtained by joining the point  $C_2 = 0.915$  with the point  $b^2/n^2 R(h+t) = 5.36$ . A straight line joining the point  $C_3 = 0.0082$  with  $q$  intersects the  $f_c/f_f$  scale at 1.13.

Hence  $f_c/f_f = 1.13$  and  $f_c = 1.13 \times 583 = 659 \text{ Hz}.$

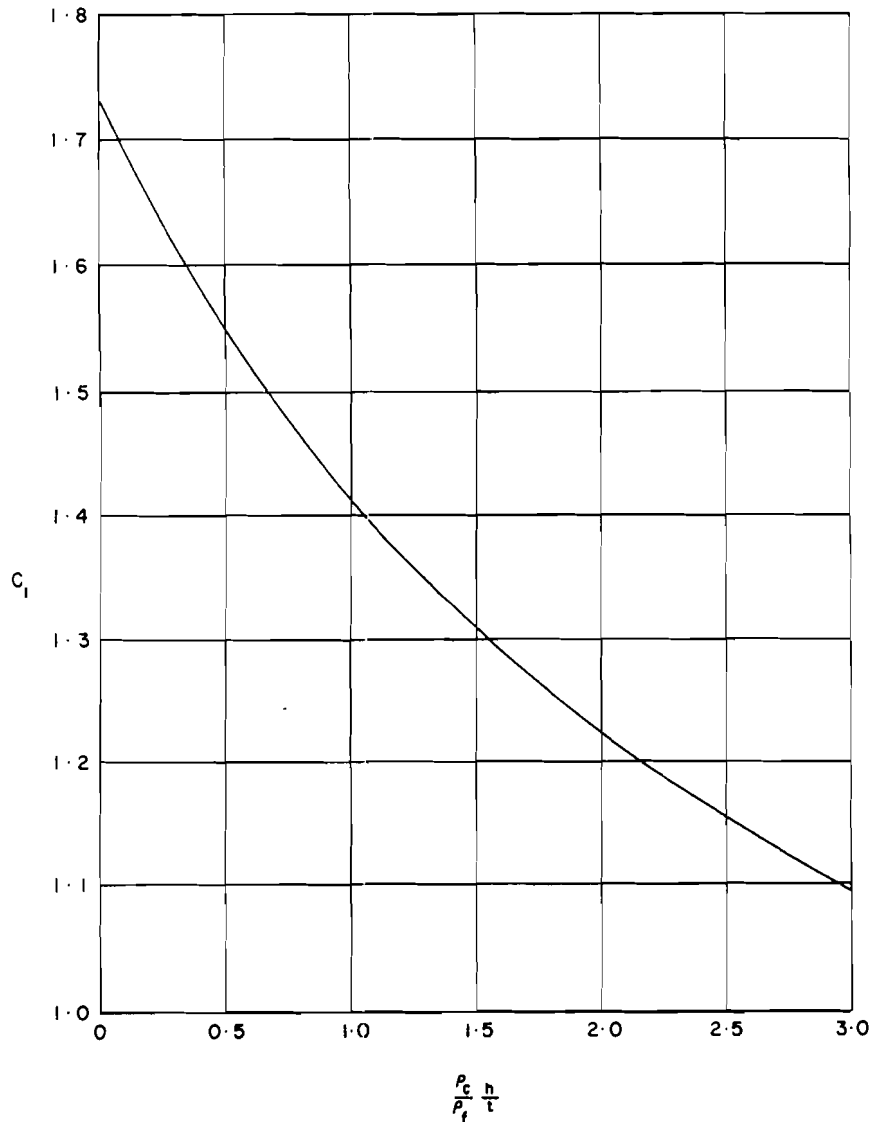


FIGURE 2.1

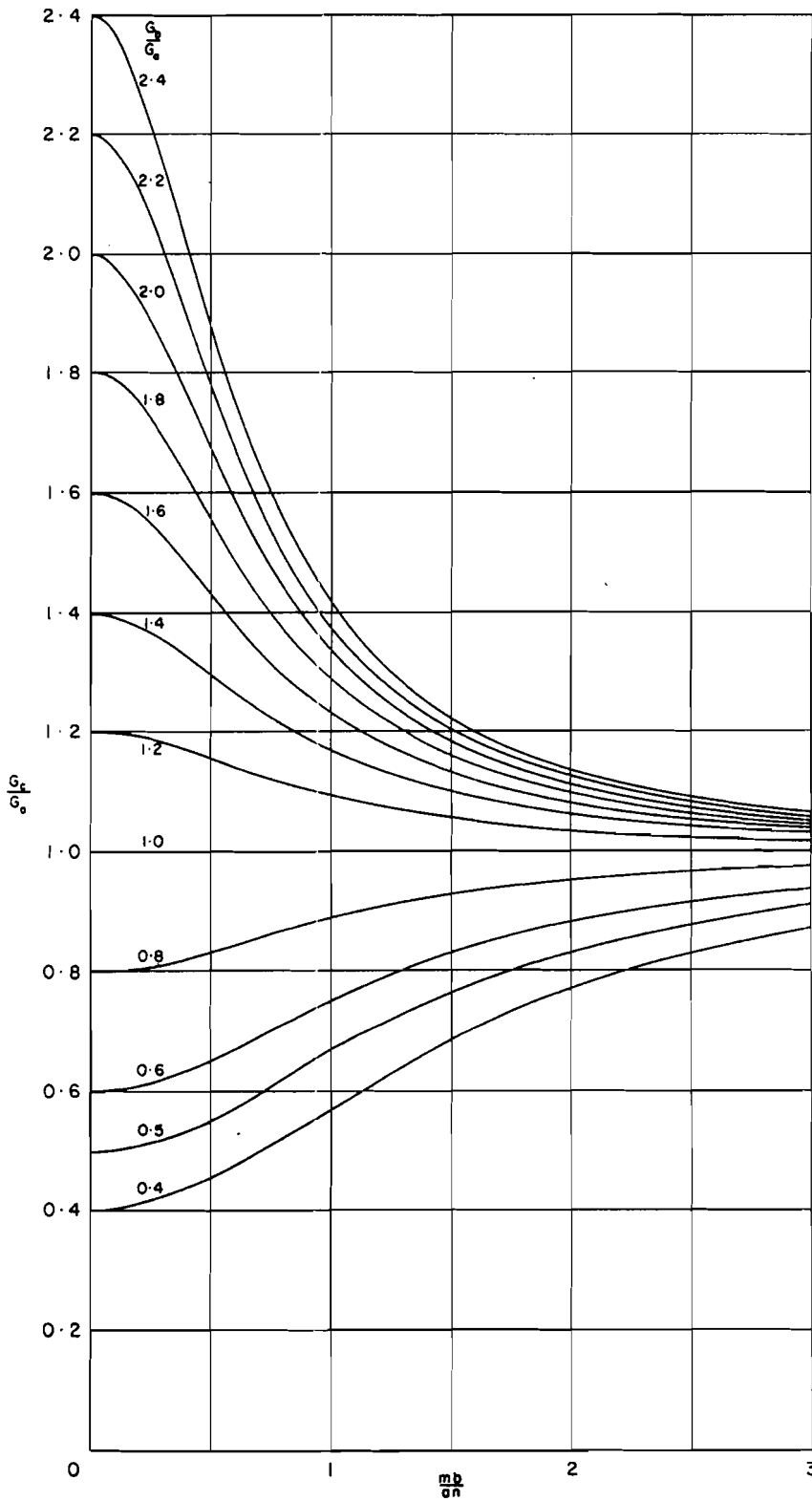


FIGURE 2.2

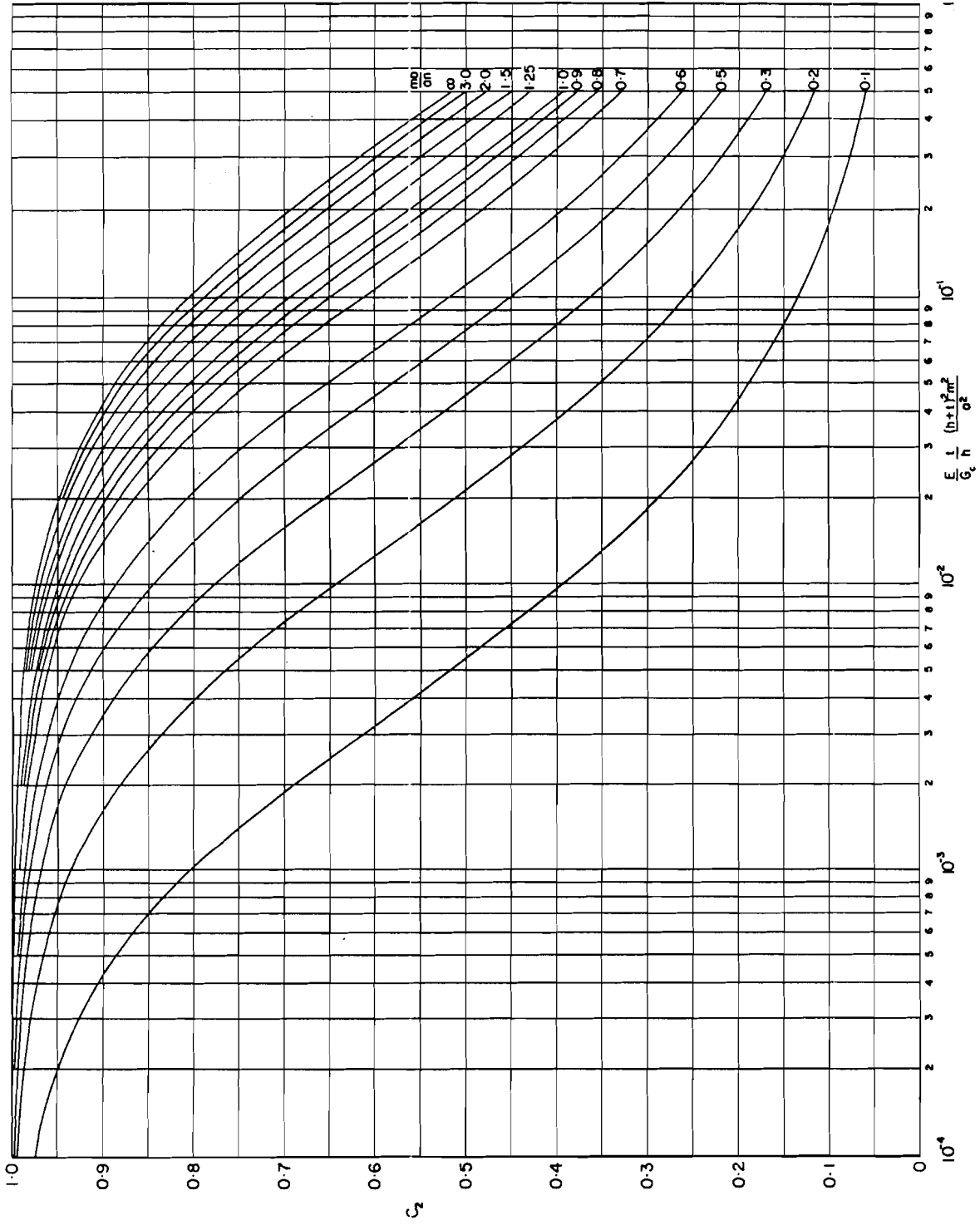


FIGURE 2.3

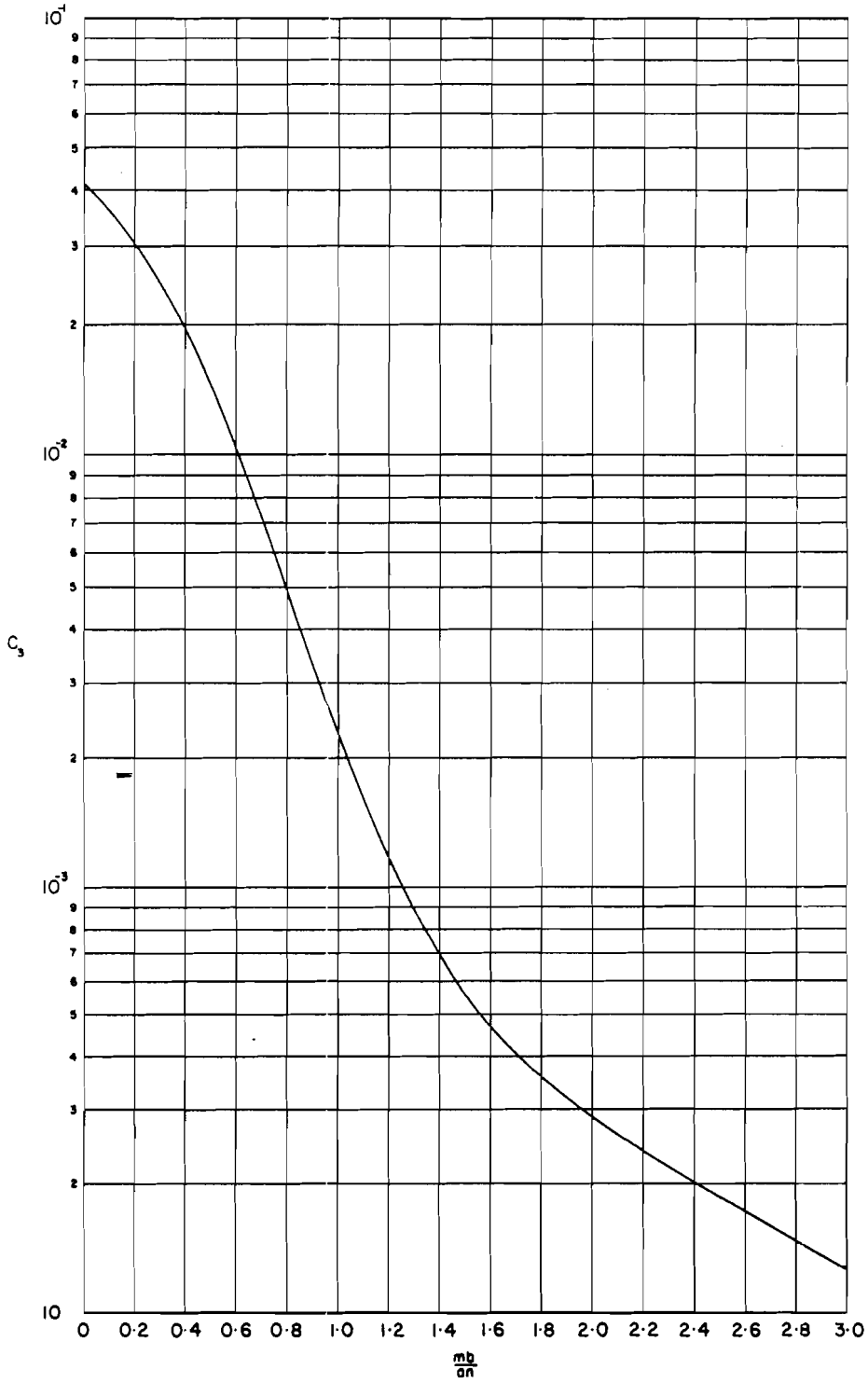


FIGURE 2.4

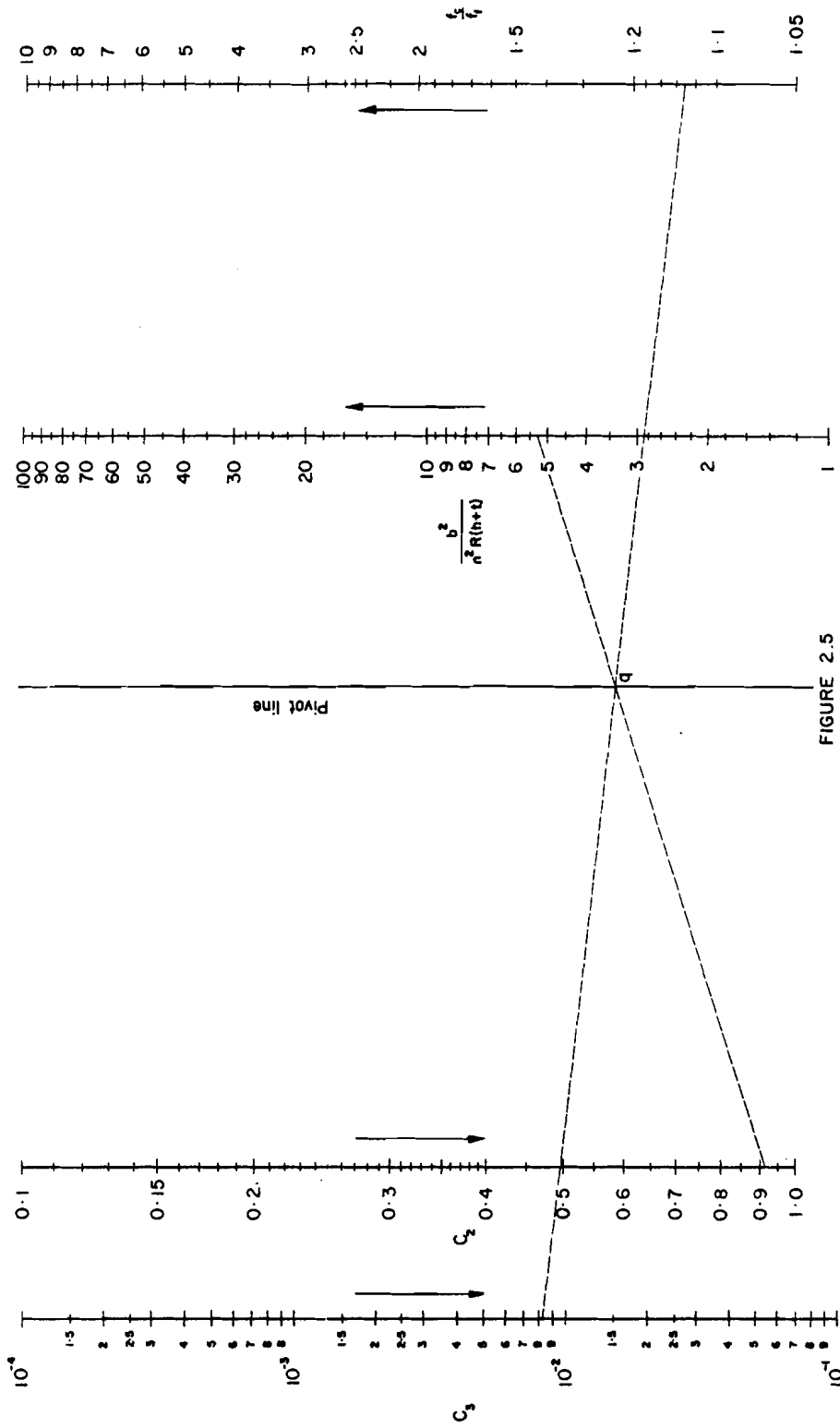


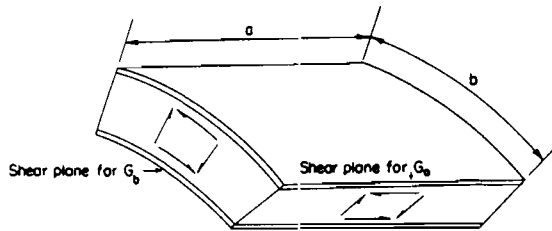
FIGURE 2.5

## Section 3

## STRESS RESPONSE OF FLAT OR SINGLY-CURVED SANDWICH PANELS WITH CORES OF ZERO FLEXURAL STIFFNESS SUBJECTED TO RANDOM ACOUSTIC LOADING

## 3.1 Notation

a	longer dimension of flat panel, or length of curved panel straight edge	m	in
b	shorter dimension of flat panel, or arc length of curved panel	m	in
E	Young's modulus of face plate material	$N/m^2$	$lbf/in^2$
$F_1, F_2$	non-dimensional parameters		
f	fundamental natural frequency of panel	Hz	c/s
$G_a, G_b$	transverse shear moduli of core defined in sketch below	$N/m^2$	$lbf/in^2$



$G_p(f)$	spectral density of acoustic pressure at frequency f	$(N/m^2)^2/Hz$	$(lbf/in^2)^2/(c/s)$
h	core thickness	m	in
$K_{1a}, K_{2a}$ $K_{1b}, K_{2b}$ $K_{1s}, K_{2s}$ $K_3$	non-dimensional parameters		
$K_\delta$	damping ratio correction factor		
$L_{ps}(f)$	spectrum level of acoustic pressure at frequency f	dB <sup>+</sup>	dB <sup>+</sup>
$P_{rms}$	r.m.s. fluctuating pressure	$N/m^2$	$lbf/in^2$
R	radius of curvature of panel	m	in
$S_{rms}$	r.m.s. stress at surface at centre of panel due to acoustic loading	$N/m^2$	$lbf/in^2$
t	face-plate thickness	m	in
$\delta$	damping ratio in the fundamental mode		
$\rho_c$	core density	$kg/m^3$	*
$\rho_f$	face-plate density	$kg/m^3$	*
$\sigma$	Poisson's ratio of face-plate material		

<sup>+</sup> The reference pressure for sound pressure level is  $20 \mu N/m^2$  ( $0.0002 \text{ dyn/cm}^2$ ).

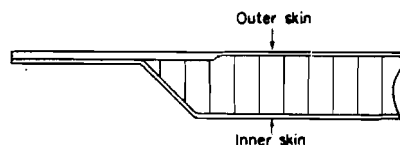
\* A density value expressed in British units as pounds per cubic inch has to be divided by 386.4 before it can be used to calculate  $(\rho_c h + 2\rho_f t)$ . (A force of 1 lbf acting on a mass of 1 lbf produces an acceleration of  $386.4 \text{ in/s}^2$ .)

### 3.2 Notes

This Section gives a method of estimating the r.m.s. stress in the face plates of a sandwich panel subjected to random acoustic loading. The panels considered are initially unstressed flat or singly-curved panels with identical face-plates. The data apply particularly to honeycomb sandwich panels but can be used for other sandwich panels provided that the core properties are such as to comply with the assumptions stated later in these notes.

The reference position for face-plate r.m.s. stress is the centre position of the panel. Stresses at other positions may be found by applying a suitable factor to the reference stress. When estimating honeycomb panel edge stresses it is necessary to consider the panel edge detail design. For a panel with reduced-thickness edges it may be assumed as a first approximation that the stresses adjacent to the edge are of the same order as the corresponding stresses at the centre. For panel edge design, the edge surface stresses should first be estimated; then, either from test or past experience, the edge design should be chosen to suit the estimated stress.

In this Section no allowance is made for the stress relief in the outside skin of a sandwich panel having crushed, or cut away, core such that the whole of the outer skin lies in the same plane. The stress relief is due to the supports restraining the panel skin in-plane extensions. Some guidance in assessing the effect of reducing the panel edge thickness on the calculated stress may be found in Reference 3.5.4. In this Reference ratios of inner and outer face-plate stresses are given for a panel mounted on rigid supports. In practical structures the compliance of the supports will reduce the stress ratios.



Sketch 2 Typical reduced thickness panel edge

It is assumed that only the fundamental mode is excited and that the panels are of shallow curvature and simply supported. The shallow curvature condition is satisfied when  $b/R < 1.5$ . In the fundamental mode the panel is assumed to vibrate with one half wave in each of the principal directions. Experimental evidence shows that the assumption of unimodal response gives good results for stresses in flat, square honeycomb panels. As the curvature and panel aspect ratio ( $a/b$ ) are increased it is likely that the effect of higher order modes will be increased. Stresses estimated for panels having  $b/R > 0.4$ , or  $0.57 > a/b > 2.0$ , should be treated with caution as no measured data are available to check the validity of the simple response theory for these cases. The assumption that panels have simply-supported edges is justified for conventional sandwich panel construction where the core material is crushed, or cut away, to bring the face plates together at the panel edge: tests show that for panels of this type the fundamental natural frequency is close to the simply-supported panel value.

This Section may be used for panels having fixed edges if an effective value is used for panel dimension  $a$ . As a first approximation it is recommended that the effective length should be the length of the simply-supported panel having the same fundamental natural frequency as the fixed-edge panel. It should be noted that experimental data are not available for comparison with calculated fixed-edge panel r.m.s. stresses so stresses calculated in this way should be treated with caution.

The core is assumed to have zero flexural stiffness and to be isotropic, although a moderate degree of orthotropy, i.e.  $1/3 < G_a/G_b < 3$ , can be taken into account. It is also assumed that the orthotropic core carries no in-plane loading, but carries all the transverse shear. The shear moduli of the core can be obtained from manufacturers' data, test or, in the case of honeycomb cores, by calculation. A suitable test method is described in Reference 3.5.8 and a calculation method for hexagonal honeycomb cores is given in Reference 3.5.9.

In producing this Section the values of  $\sigma$  and  $\delta$  have been assumed to be 0.3 and 0.019 respectively. This value of the damping ratio in the fundamental mode is typical for bonded aluminium alloy honeycomb panels. However, r.m.s. stresses at different values of damping ratio may be found using the correction factor  $K_\delta$  which is plotted against  $\delta$  in Figure 3.14.

In Appendix 3A a computer program is described which calculates both natural frequencies and stress response to acoustic loading. Sub-routines are given for both the frequency and stress calculations.

### 3.3 Calculation Procedure

3.3.1 The procedure for estimating  $S_{rms}$  in a general case is as follows

- (1) Estimate the fundamental natural frequency of the panel using Section 2.

- (ii) Obtain the value of spectrum level of acoustic pressure  $L_{ps}(f)$  at the calculated frequency. If only the band pressure level is known, it is first corrected to pressure spectrum level (unit bandwidth) using Reference 3.5.5.
- (iii) Evaluate  $a/b$  and, from Figure 1, read the value of  $K_1$  appropriate to the direction in which the r.m.s. stress is required (see Derivation).
- (iv) Evaluate  $G_b/G_a$  and  $G_a a^2 h / \{Et(t+h)^2\}$  and from Figures 3.2 to 3.6 or Figures 3.7 to 3.11, depending on the direction in which the stress is required (see Derivation), read the appropriate value of  $K_2$ . The Figure used within these two groups depends on the value of  $G_b/G_a$ .
- (v) Evaluate  $a/R$  and  $\{(h/2)+t\}/a$  and calculate  $K_3$  from:
- $$K_3 = \left| \frac{a}{R} K_{1s} \pm \left( \frac{h}{2} + t \right) \frac{K_{2s}}{a} \right|.$$
- The sign chosen for the product including  $K_2$  is dependent on the panel surface for which the r.m.s. stress is required (see Derivation).
- (vi) Evaluate the parameter  $E/\{a(\rho_c h + 2\rho_f t)\}$  and from the nomograph (Figures 3.12 or 3.13) obtain the value of  $S_{rms}$ . The nomographs are entered at a value of  $L_{ps}(f)$ , each quadrant being used in turn in the direction indicated through ranges of  $E/\{a(\rho_c h + 2\rho_f t)\}$ ,  $K_3$  and  $f$ . Figure 3.13 is an extension of the range of  $L_{ps}(f)$  given in Figure 3.12.
- (vii) For values of  $\delta$  other than 0.019, factor the estimated value of  $S_{rms}$  by  $K_\delta$  obtained from Figure 3.14. The value of  $\delta = 0.019$  is typical for bonded aluminium alloy honeycomb panels.

### 3.3.2 Note on the units of spectral density of acoustic pressure

Within the nomograph the spectrum sound pressure level is converted into the spectral density of acoustic pressure. The spectrum sound pressure level is converted into the root mean square fluctuating pressure in units of  $(N/m^2)/Hz$  (see expression below or Reference 3.5.6) and then squared giving a value in units of  $(N/m^2)^2/Hz^2$ . Since unit bandwidth is used this is numerically equal to the spectral density of acoustic pressure  $G_p(f)$  in units of  $(N/m^2)^2/Hz$ .

$$L_{ps}(f) = 20(\log_{10} P_{rms} + 4.70)$$

If  $L_{ps}(f)$  is required in British units of  $(lbf/in^2)^2/(c/s)$  it is given by

$$L_{ps}(f) = 20(\log_{10} P_{rms} + 8.54).$$

### 3.4 Comparison with Measured Data

Figures 3.15 and 3.16 show a comparison of estimated and measured face-plate r.m.s. stress at the centre of sandwich panels. In estimating stresses for Figure 3.15 the fundamental natural frequency calculated using Section 2 was used, and the value of damping ratio was taken to be 0.019. For estimated stresses in Figure 3.16 measured values of fundamental natural frequency and corresponding damping ratio were used.

All data used in these comparisons are for panels having crushed or cutaway cores at the edge attachment positions. No allowance has been made for stress relief due to the rigidity of the supports. In all cases the highest measured panel centre stress is compared with the equivalent highest calculated principal stress.

### 3.5 Derivation and References

#### Derivation

The expression for r.m.s. stress is  $S_{rms} = \frac{0.29K_3EK\delta}{a(\rho_c h + 2\rho_f t)f^{3/2}} \left\{ G_p(f) \right\}^{1/2}$

$$\text{where } K_3 = \left| \frac{a}{R} K_{1s} + \left( \frac{h}{2} + t \right) \frac{K_{2s}}{a} \right| .$$

- (i) For surface stresses parallel to the panel side of length  $a$   $K_{1s} = K_{1a}$  and  $K_{2s} = K_{2a}$  where

$$K_{1a} = -\frac{2}{F_1} (1-\sigma) \left\{ \left( \frac{a}{b} \right)^2 - \sigma \right\} + \sigma - \sigma \left( \frac{a}{b} \right) \frac{2}{F_1} \left\{ \sigma(1+\sigma) - 2 - \left( \frac{a}{b} \right)^2 (1-\sigma) \right\}$$

$$\text{and } K_{2a} = \frac{2\pi^3}{F_2} \left\{ 2\pi \left( \frac{G_b}{G_a} \right) \left[ 1 + \left( \frac{a}{b} \right)^2 \sigma \right] + \frac{\pi^3 Et(t+h)^2}{2G_a a^2 h(1-\sigma^2)} \times \right. \\ \left. \left\{ 2 \left( \frac{a}{b} \right)^2 \left[ 1 + \sigma \left( \frac{G_b}{G_a} \right) \right] + (1-\sigma) \left[ 1 + \left( \frac{a}{b} \right)^4 \left( \frac{G_b}{G_a} \right) \sigma \right] - \left( \frac{a}{b} \right)^2 (1+\sigma) \left[ \left( \frac{G_b}{G_a} \right) + \sigma \right] \right\} \right\} .$$

- (ii) For surface stresses parallel to the panel side of length  $b$   $K_{1s} = K_{1b}$  and  $K_{2s} = K_{2b}$  where

$$K_{1b} = -\frac{2\sigma}{F_1} (1-\sigma) \left\{ \left( \frac{a}{b} \right)^2 - \sigma \right\} + 1 - \frac{2}{F_1} \left( \frac{a}{b} \right) \left\{ \sigma(1+\sigma) - 2 - \left( \frac{a}{b} \right)^2 (1-\sigma) \right\}$$

$$\text{and } K_{2b} = \frac{2\pi^3}{-F_2} \left\{ 2\pi \left( \frac{G_b}{G_a} \right) \left[ \sigma + \left( \frac{a}{b} \right)^2 \right] + \frac{\pi^3 Et(t+h)^2}{2G_a a^2 h(1-\sigma^2)} \times \right. \\ \left. \left\{ 2 \left( \frac{a}{b} \right)^2 \left[ \sigma + \left( \frac{G_b}{G_a} \right) \right] + (1-\sigma) \left[ \sigma + \left( \frac{a}{b} \right)^4 \left( \frac{G_b}{G_a} \right) \right] - \left( \frac{a}{b} \right)^2 (1+\sigma) \left[ 1 + \sigma \left( \frac{G_b}{G_a} \right) \right] \right\} \right\}$$

$$F_1 = \left( \frac{a}{b} \right)^2 (1+\sigma)^2 - \left[ 2 \left( \frac{a}{b} \right)^2 + 1 - \sigma \right] \left[ 2 + \left( \frac{a}{b} \right)^2 (1-\sigma) \right]$$

$$F_2 = 4\pi^2 \left( \frac{G_b}{G_a} \right) + \frac{\pi^4 Et(t+h)^2}{G_a a^2 h(1-\sigma^2)} \left\{ 2 \left( \frac{a}{b} \right)^2 + 2 \left( \frac{G_b}{G_a} \right) \right. \\ \left. + (1-\sigma) \left[ 1 + \left( \frac{a}{b} \right)^2 \left( \frac{G_b}{G_a} \right) \right] \right\} - F_1 \left\{ \frac{\pi^3 Et(t+h)^2}{2G_a a^2 h(1-\sigma^2)} \right\}^2 .$$

In the equation for  $K_3$  the minus sign, in front of the final product, is used for surface stress on the convex side of the panel and the plus sign for the surface stress on the concave side of the panel.

- 3.5.1 Ballentine, J.R. et al. Sonic fatigue in combined environment. Air Force Flight Dynamics Lab., tech. Rep. AFFDL-TR-66-7, May 1966.
- 3.5.2 Ballentine, J.R. et al. Refinement of sonic fatigue structural design criteria. Air Force Flight Dynamics Lab., tech. Rep. AFFDL-TR-67-156, November 1967.
- 3.5.3 Jacobson, M.J. Stress and deflection of honeycomb panels loaded by spatially uniform white noise, AIAA Journal, Vol.6, No.8, pp.1503-1510, August 1968.

#### References

- 3.5.4 Sweers, J.E. Prediction of response and fatigue life of honeycomb sandwich panels subjected to acoustic excitation. Acoustic fatigue in aerospace structures. Syracuse University Press, 1965.
- 3.5.5 - Bandwidth correction. Engineering Sciences Data Item No. 66016, February 1966.
- 3.5.6 - The relation between sound pressure level and r.m.s. fluctuating pressure. Engineering Sciences Data Item No. 66018, February 1966.
- 3.5.7 - Natural frequencies of uniform flat plates. Engineering Sciences Data Item No. 66019, February 1966.
- 3.5.8 - Experimental determination of the shear and flexural stiffness of a sandwich panel. Engineering Sciences Data Item No. 66025, June 1966.
- 3.5.9 - Modulus of rigidity of sandwich panels with hexagonal cell cores. Engineering Sciences Data Item No. 67022, March 1967.

#### 3.6 Example

It is required to estimate the r.m.s. stress on the face plates at the centre of a simply-supported honeycomb sandwich panel subject to jet noise. The variation of sound pressure level over a range of frequencies is given in the table, sound pressure level being 1/3 octave band levels.

Sound pressure level dB	152	155	154	150
Frequency Hz	200	500	1000	2000

The panel has the following dimensions and material properties:

$$\begin{aligned}
 a &= 450 \text{ mm}, & b &= 300 \text{ mm}, & R &= 1600 \text{ mm}, \\
 h &= 10 \text{ mm}, & t &= 0.5 \text{ mm}, & \sigma &= 0.3, \\
 E &= 70\,400 \text{ MN/m}^2, & G_a &= 141 \text{ MN/m}^2, & G_b &= 212 \text{ MN/m}^2, \\
 \rho_f &= 2660 \text{ kg/m}^3, & \rho_c &= 64 \text{ kg/m}^3.
 \end{aligned}$$

From Section 2 the fundamental natural frequency of the panel is 659 Hz.

By interpolation from the table the 1/3 octave band pressure level at 659 Hz is 154.9 dB.

From Reference 3.5.5,

$$L_{ps}(f) = 154.9 - 21.7 = 133.2 \text{ dB.}$$

With  $a/b = 1.5$ , from Figure 3.1

$$K_{1a} = 0.290 \quad \text{and} \quad K_{1b} = 0.408.$$

$$\text{Now } G_b/G_a = 1.5$$

$$\text{and } \frac{G_a a^2 h}{Et(t+h)^2} = \frac{141 \times 10^6 \times 0.45^2 \times 0.01}{70\,400 \times 10^6 \times 0.0005(0.0005 + 0.01)^2} = 73.6.$$

Therefore from Figure 3.5,  $K_{2a} = 13.5$  and from Figure 3.10  $K_{2b} = 21.2$ .

$$\text{Also } \frac{a}{R} = \frac{0.45}{1.60} = 0.281 \quad \text{and} \quad \frac{(\frac{h}{2}+t)}{a} = \frac{\frac{0.01}{2} + 0.0005}{0.45} = 0.0122.$$

From the equations in the Derivation, Section 3.5, the values of  $K_3$  required to determine the r.m.s. stress parallel to side  $a$  are given by

(i) on the concave face-plate surface

$$\begin{aligned} K_3 &= \left| \frac{a}{R} K_{1a} + \left(\frac{h}{2}+t\right) \frac{K_{2a}}{a} \right| \\ &= \left| 0.281 \times 0.290 + 0.0122 \times 13.5 \right| = 0.246 \end{aligned}$$

and (ii) on the convex face-plate surface

$$\begin{aligned} K_3 &= \left| \frac{a}{R} K_{1a} - \left(\frac{h}{2}+t\right) \frac{K_{2a}}{a} \right| \\ &= \left| 0.281 \times 0.290 - 0.0122 \times 13.5 \right| = 0.083 \end{aligned}$$

the values of  $K_3$  required to determine the r.m.s. stress parallel to side  $b$  are given by

(i) on the concave face-plate surface

$$\begin{aligned} K_3 &= \left| \frac{a}{R} K_{1b} + \left(\frac{h}{2}+t\right) \frac{K_{2b}}{a} \right| \\ &= \left| 0.281 \times 0.408 + 0.0122 \times 21.2 \right| = 0.373 \end{aligned}$$

and (ii) on the convex face-plate surface

$$\begin{aligned} K_3 &= \left| \frac{a}{R} K_{1b} - \left(\frac{h}{2}+t\right) \frac{K_{2b}}{a} \right| \\ &= \left| 0.281 \times 0.408 - 0.0122 \times 21.2 \right| = 0.144 \end{aligned}$$

$$\text{then } \frac{E}{a(\rho_c h + 2\rho_f t)} = \frac{70\,400 \times 10^6}{0.450 \times (64 \times 0.01 + 2 \times 2660 \times 0.0005)} = 47.4 \times 10^9 \text{ s}^{-2}.$$

From Figure 3.13, entering the nomograph at 133.2 dB the stresses in the face plates are shown in the table.

	$S_{\text{rms}}$ parallel to side $a$ (MN/m <sup>2</sup> )	$S_{\text{rms}}$ parallel to side $b$ (MN/m <sup>2</sup> )
concave surface	18.3	27.7
convex surface	6.2	10.7

Therefore the resultant stress on the panel concave surface ( $\delta = 0.019$ ) is

$$\sqrt{18.3^2 + 27.7^2} = 33.2 \text{ MN/m}^2,$$

and the resultant stress on the panel convex surface ( $\delta = 0.019$ ) is

$$\sqrt{6.2^2 + 10.7^2} = 12.4 \text{ MN/m}^2.$$

From Figure 3.14, for  $\delta = 0.03$ ,  $K_\delta = 0.796$ .

Hence the r.m.s. stress at the centre of the panel on the concave surface is  $33.2 \times 0.796 = 26.4 \text{ MN/m}^2$  and on the convex surface is  $12.4 \times 0.796 = 9.87 \text{ MN/m}^2$ .

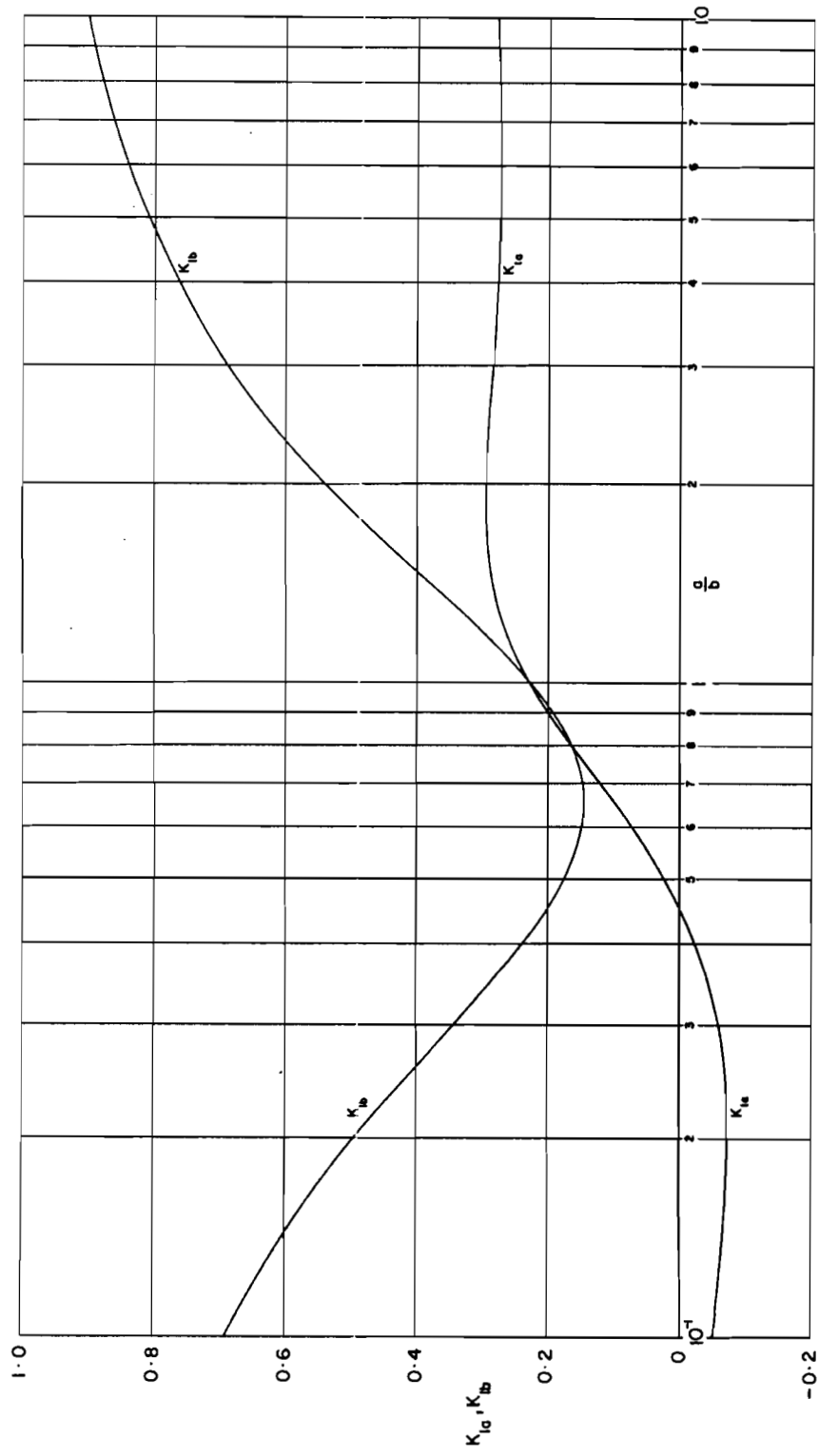


FIGURE 3I CURVATURE FACTOR PARAMETERS

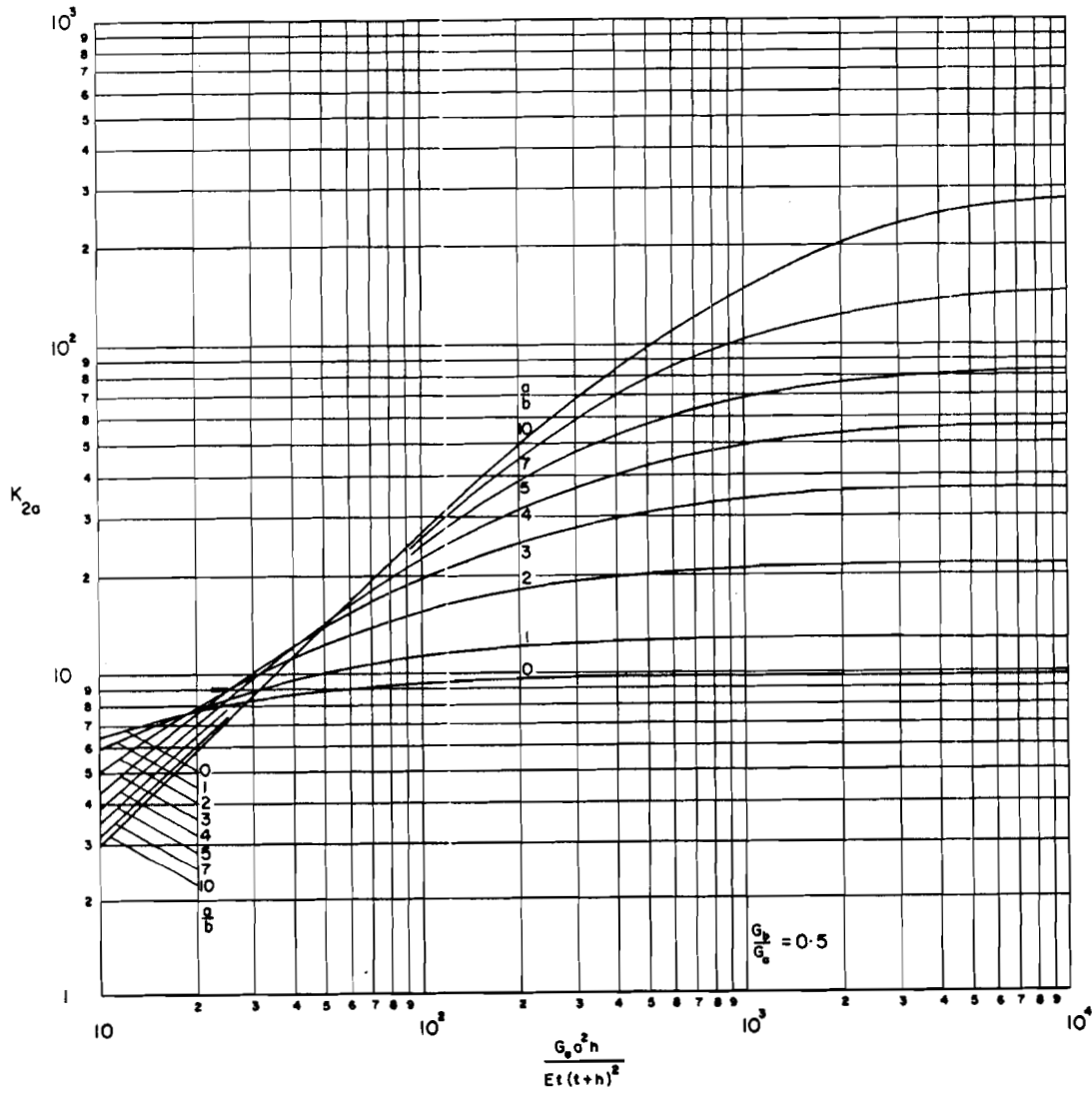


FIGURE 32. PARAMETER FOR STRESS PARALLEL TO PANEL SIDE  $\sigma$

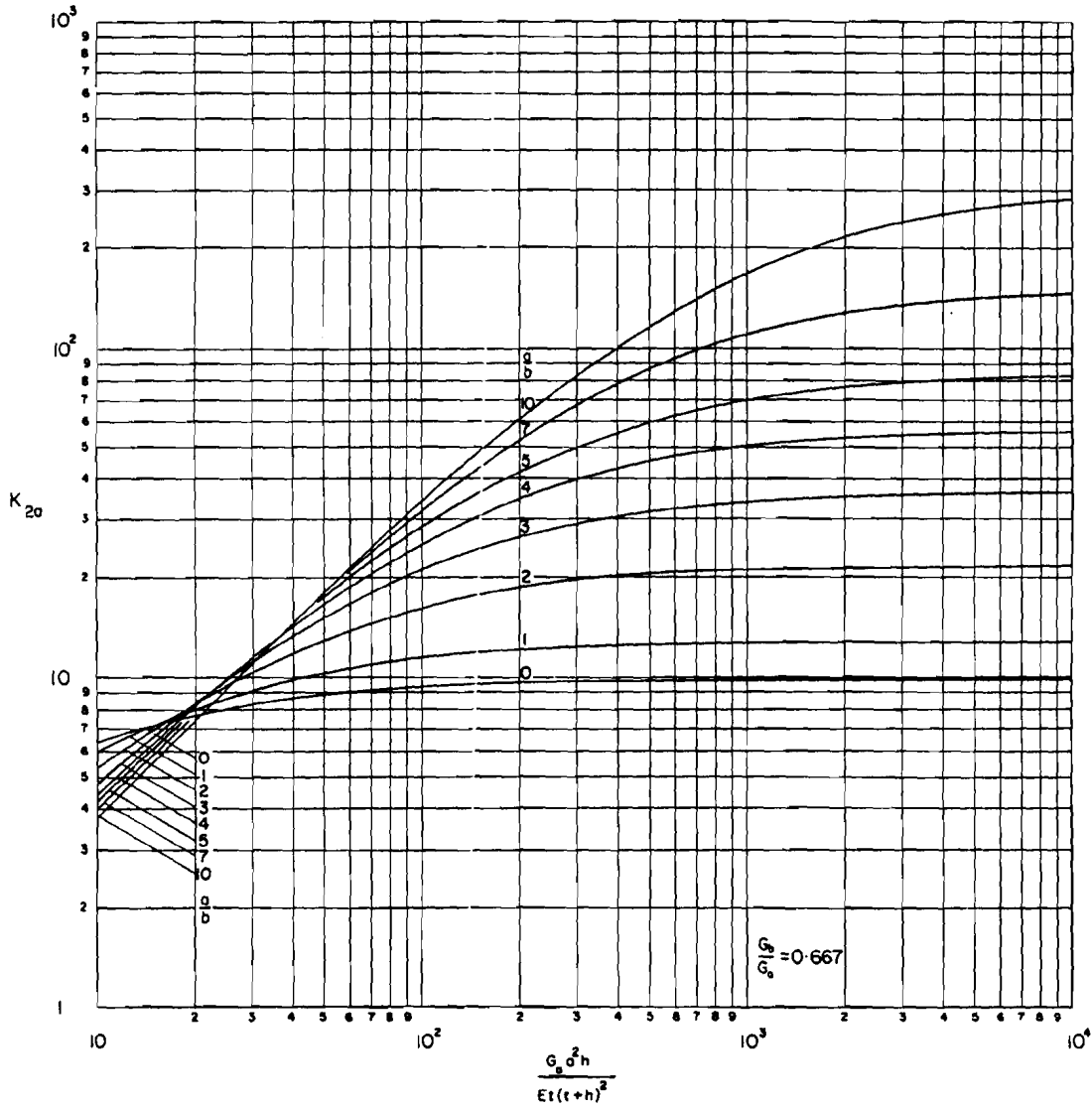


FIGURE 3.3. PARAMETER FOR STRESS PARALLEL TO PANEL SIDE a

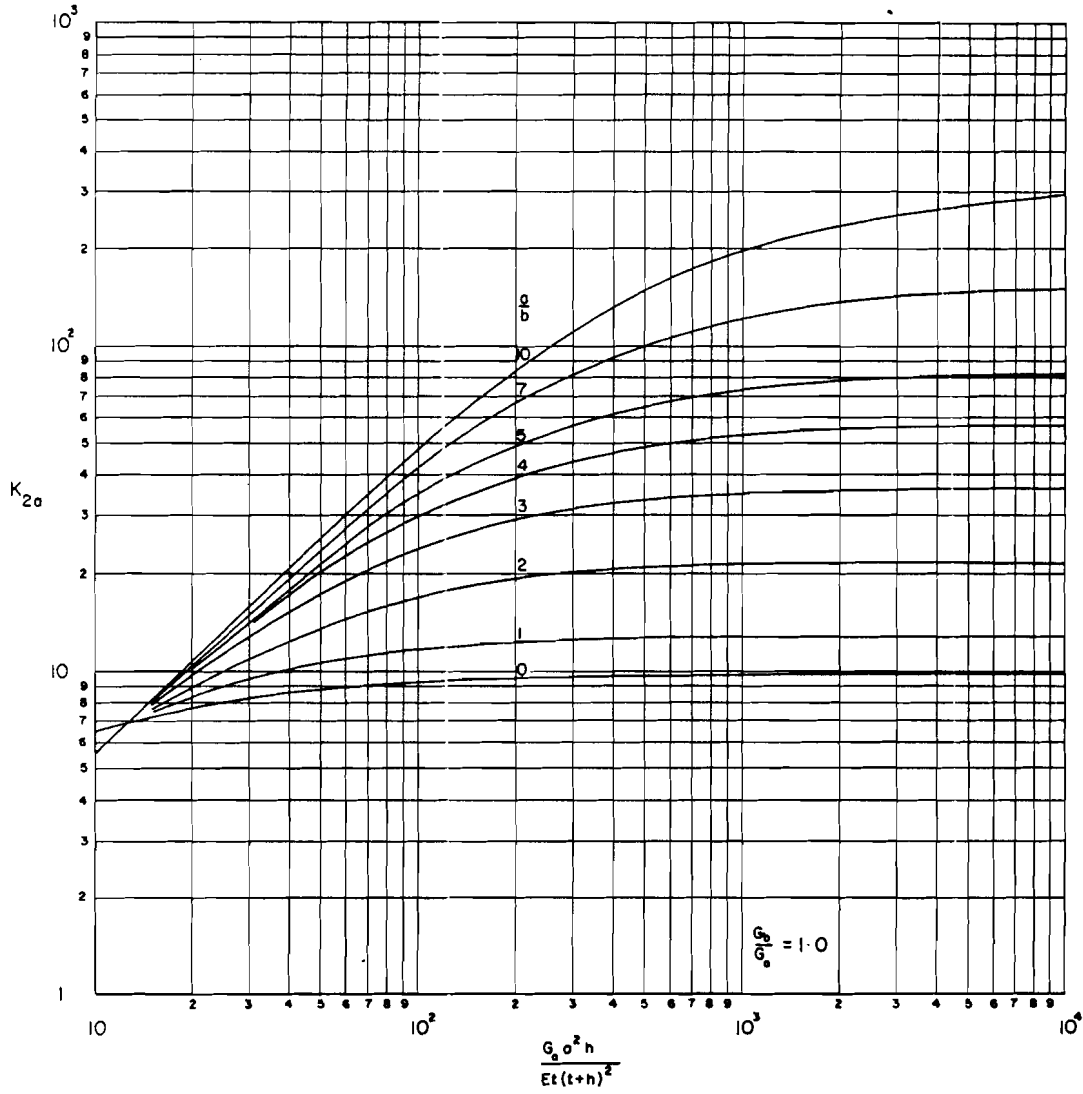


FIGURE 3.4 PARAMETER FOR STRESS PARALLEL TO PANEL SIDE a

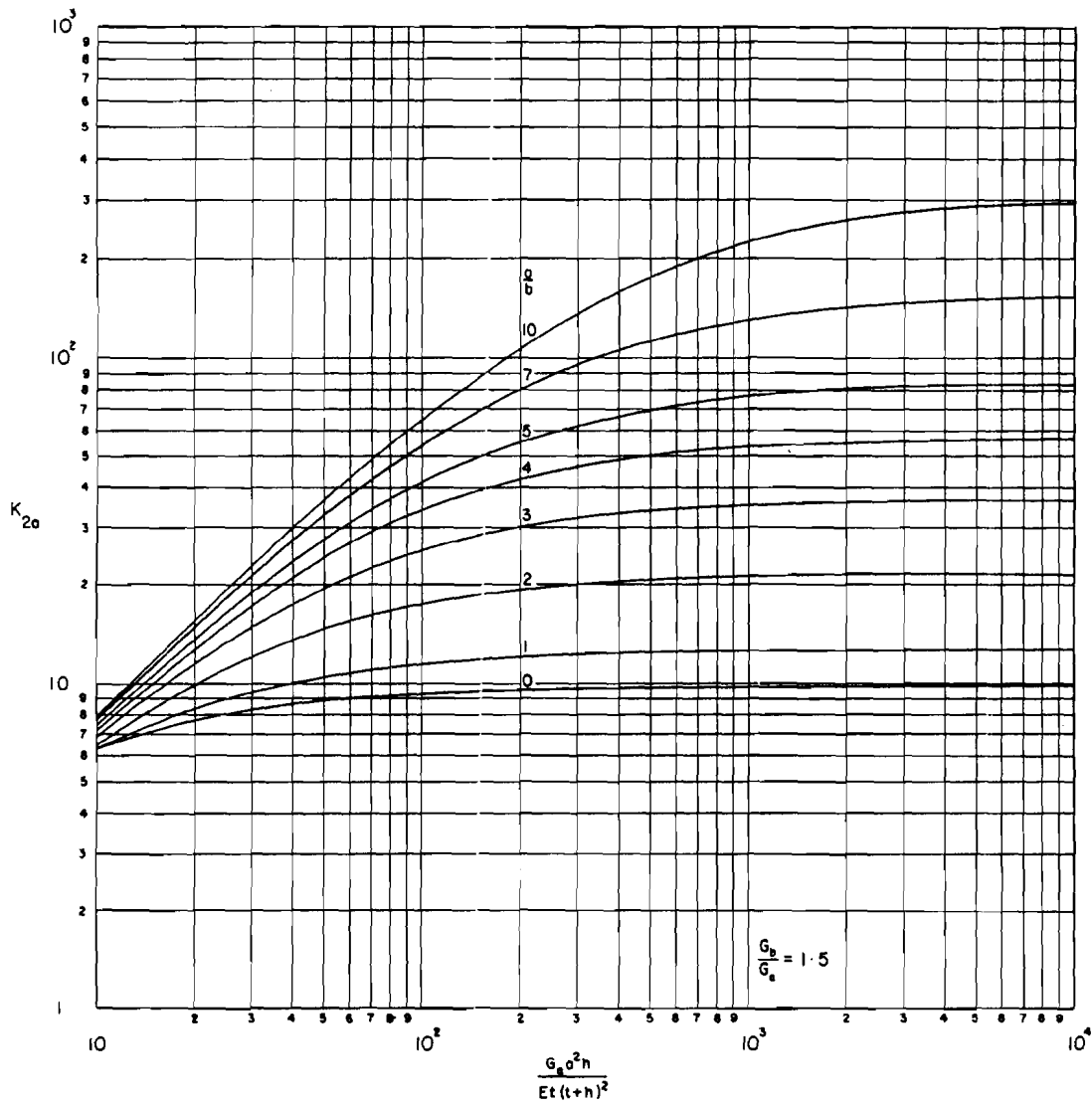


FIGURE 35. PARAMETER FOR STRESS PARALLEL TO PANEL SIDE  $\sigma$

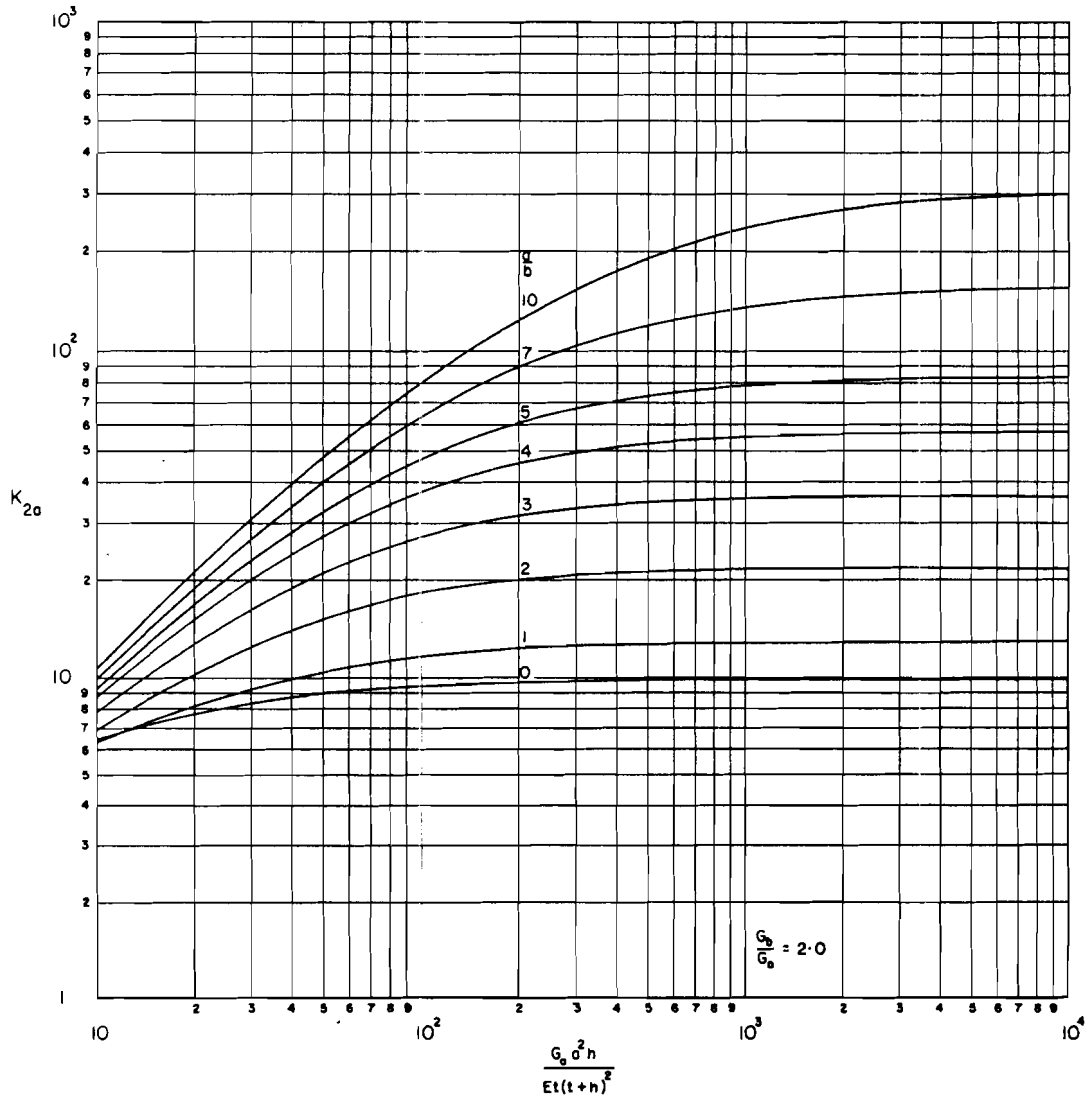


FIGURE 36. PARAMETER FOR STRESS PARALLEL TO PANEL SIDE a

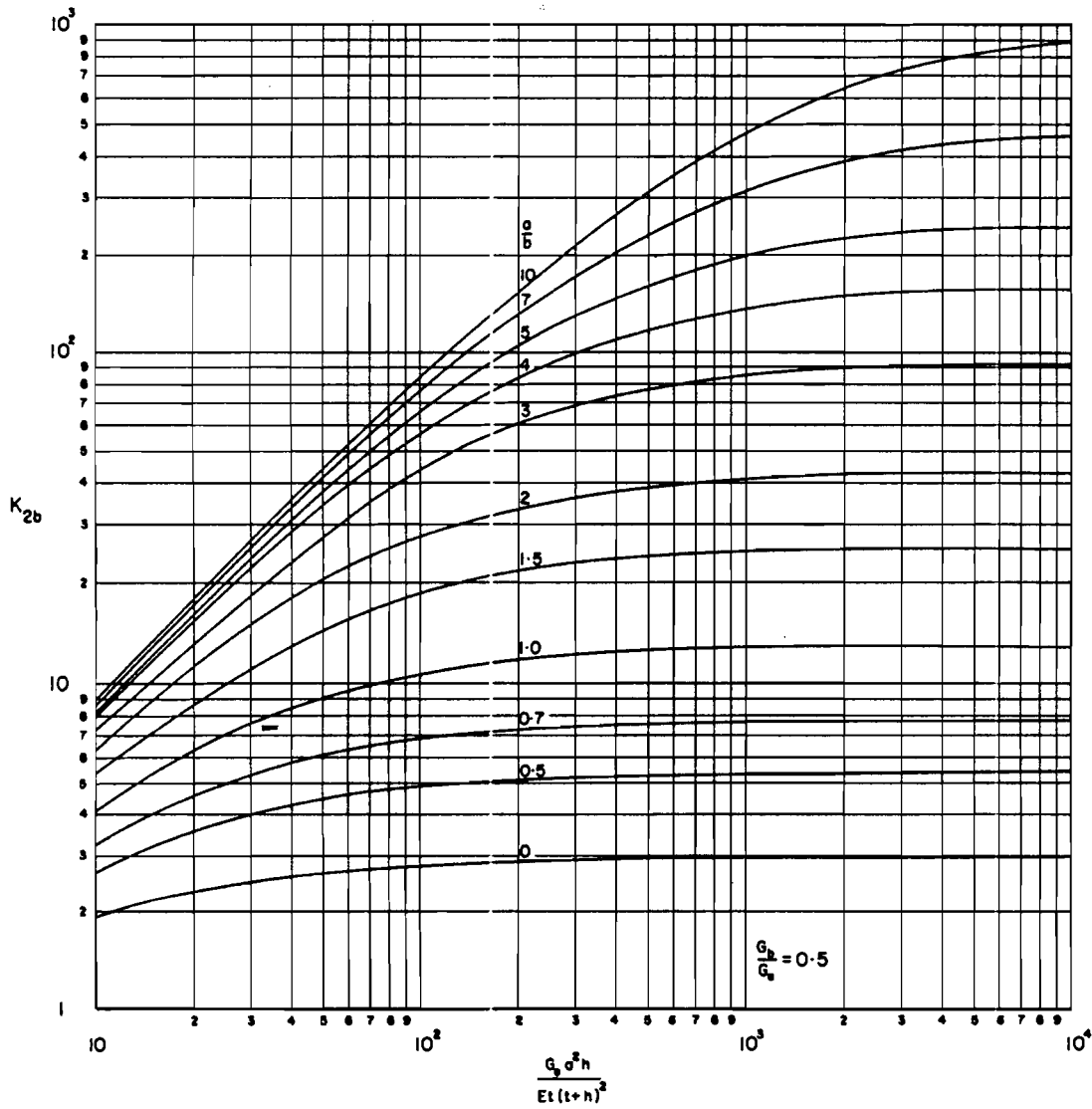


FIGURE 3.7. PARAMETER FOR STRESS PARALLEL TO PANEL SIDE b

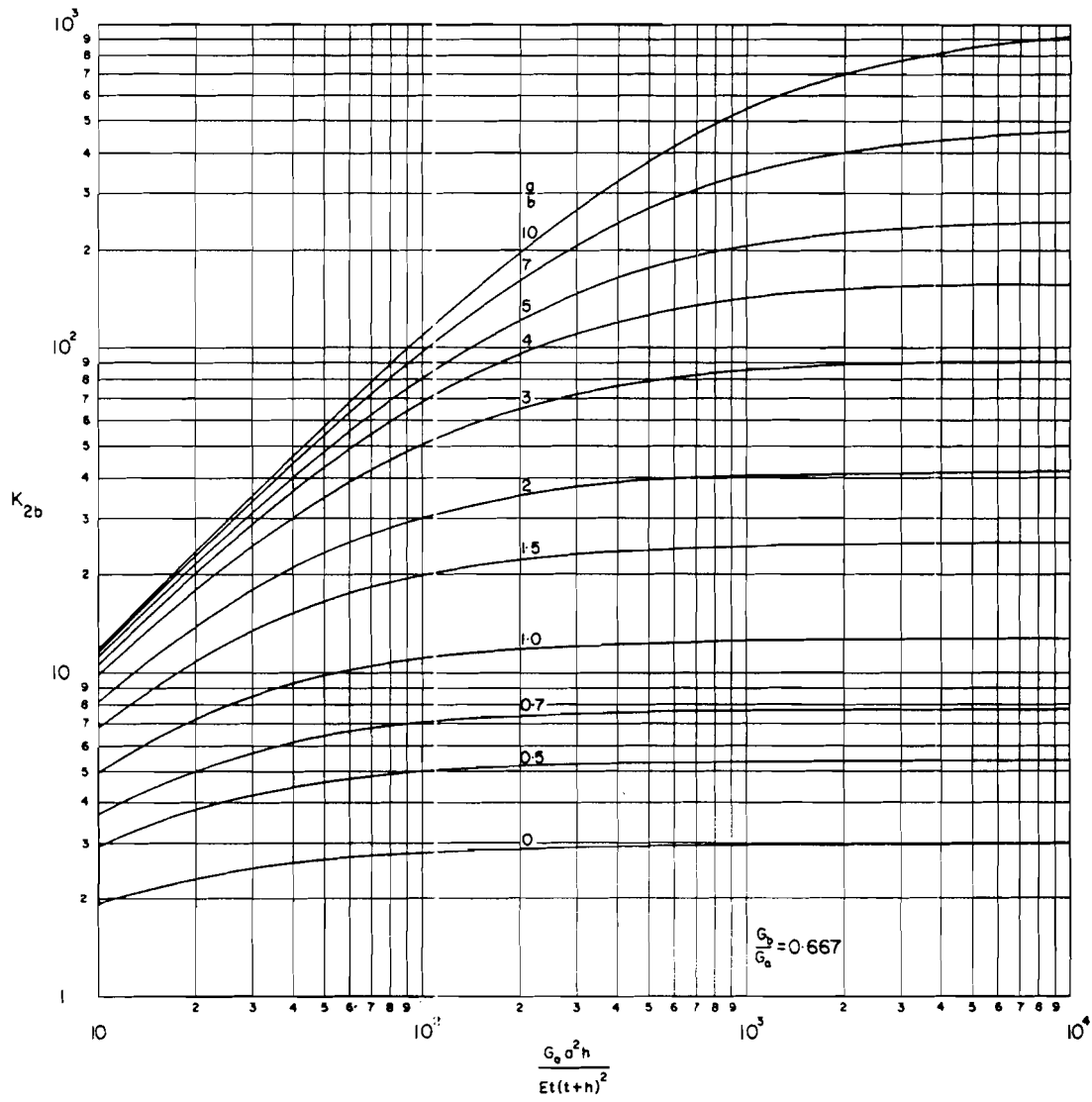


FIGURE 38. PARAMETER FOR STRESS PARALLEL TO PANEL SIDE b

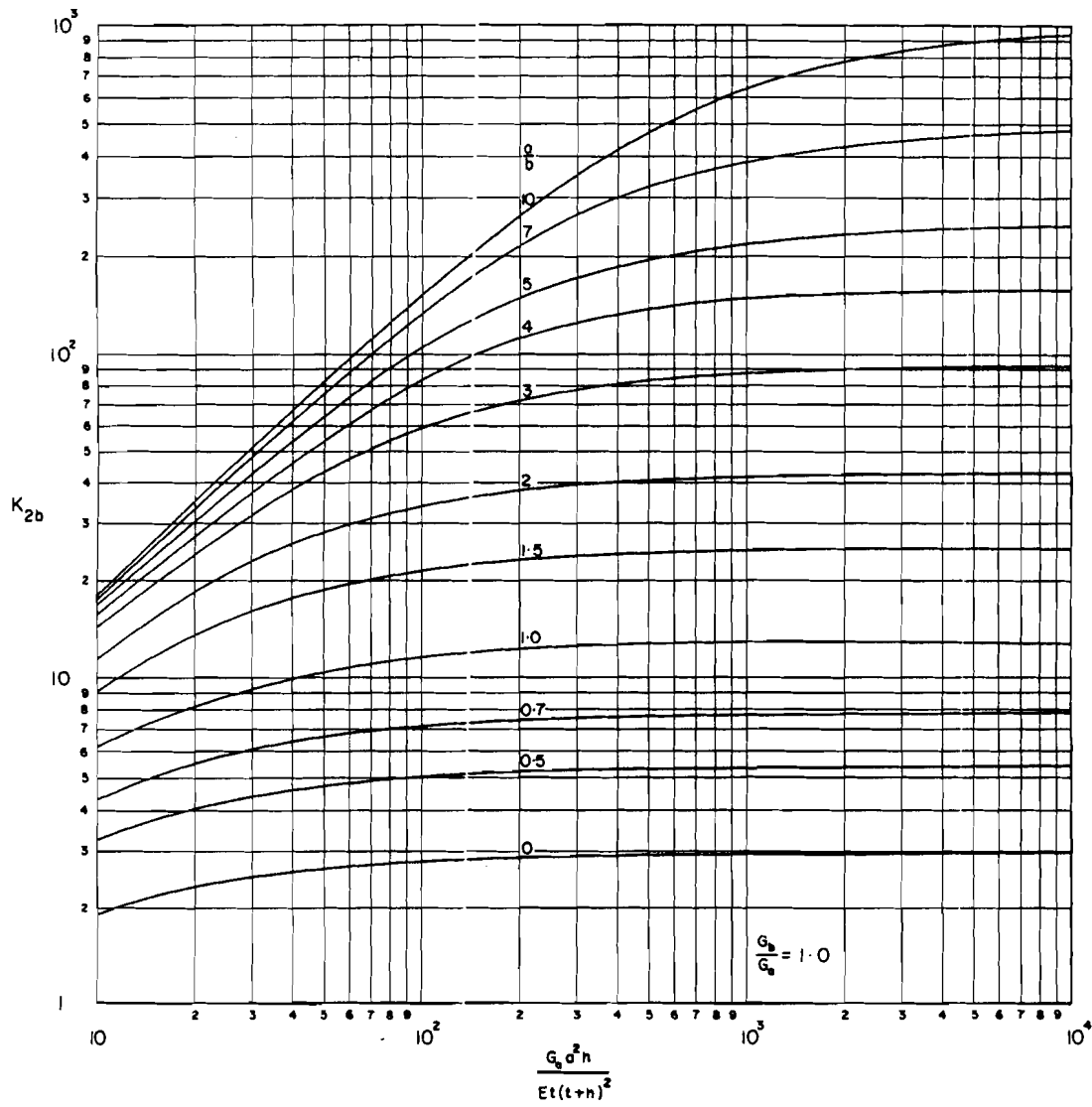


FIGURE 39 PARAMETER FOR STRESS PARALLEL TO PANEL SIDE b

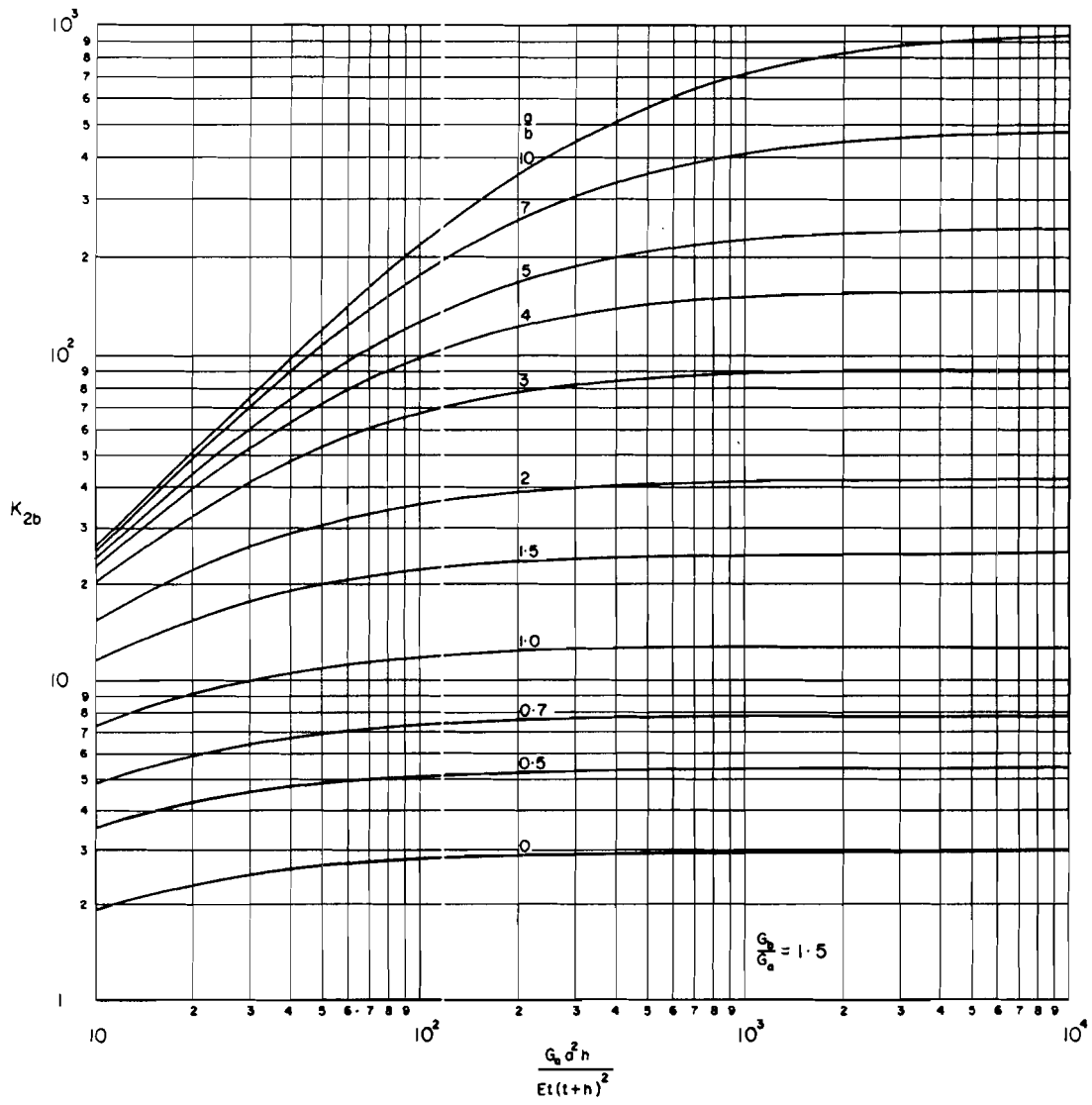


FIGURE 3.10. PARAMETER FOR STRESS PARALLEL TO PANEL SIDE b

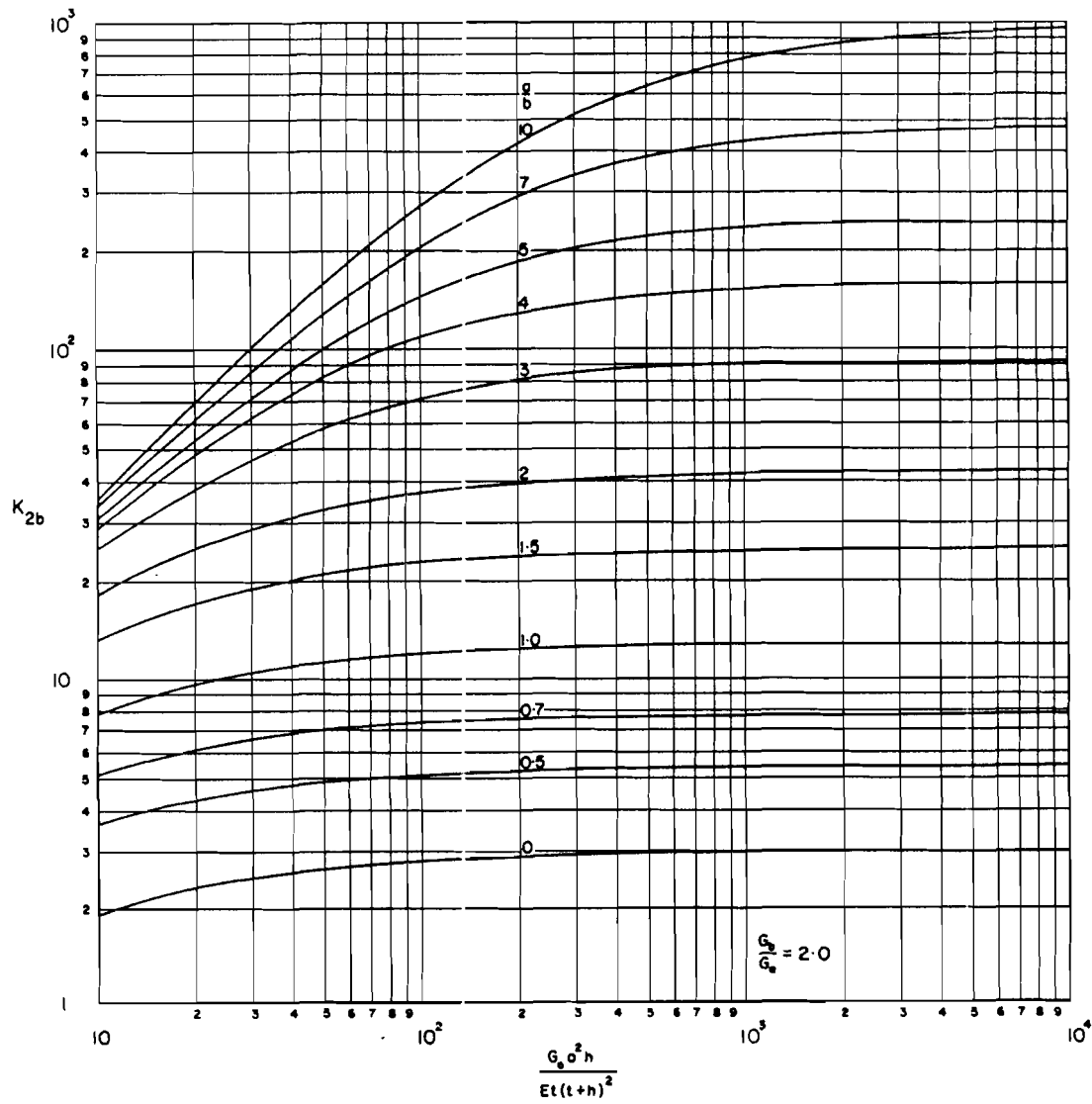


FIGURE 3.II. PARAMETER FOR STRESS PARALLEL TO PANEL SIDE b

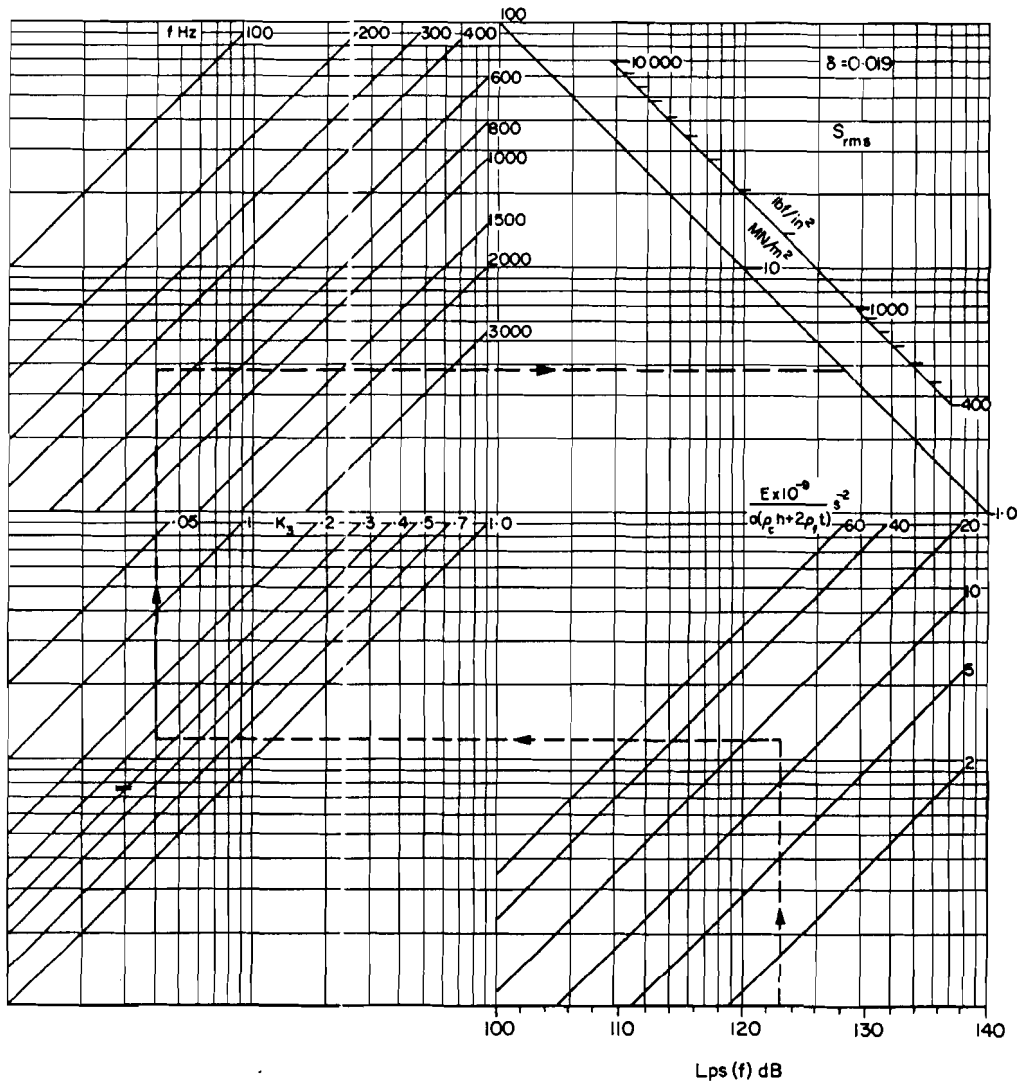


FIGURE 3.12. STRESS NOMOGRAPH

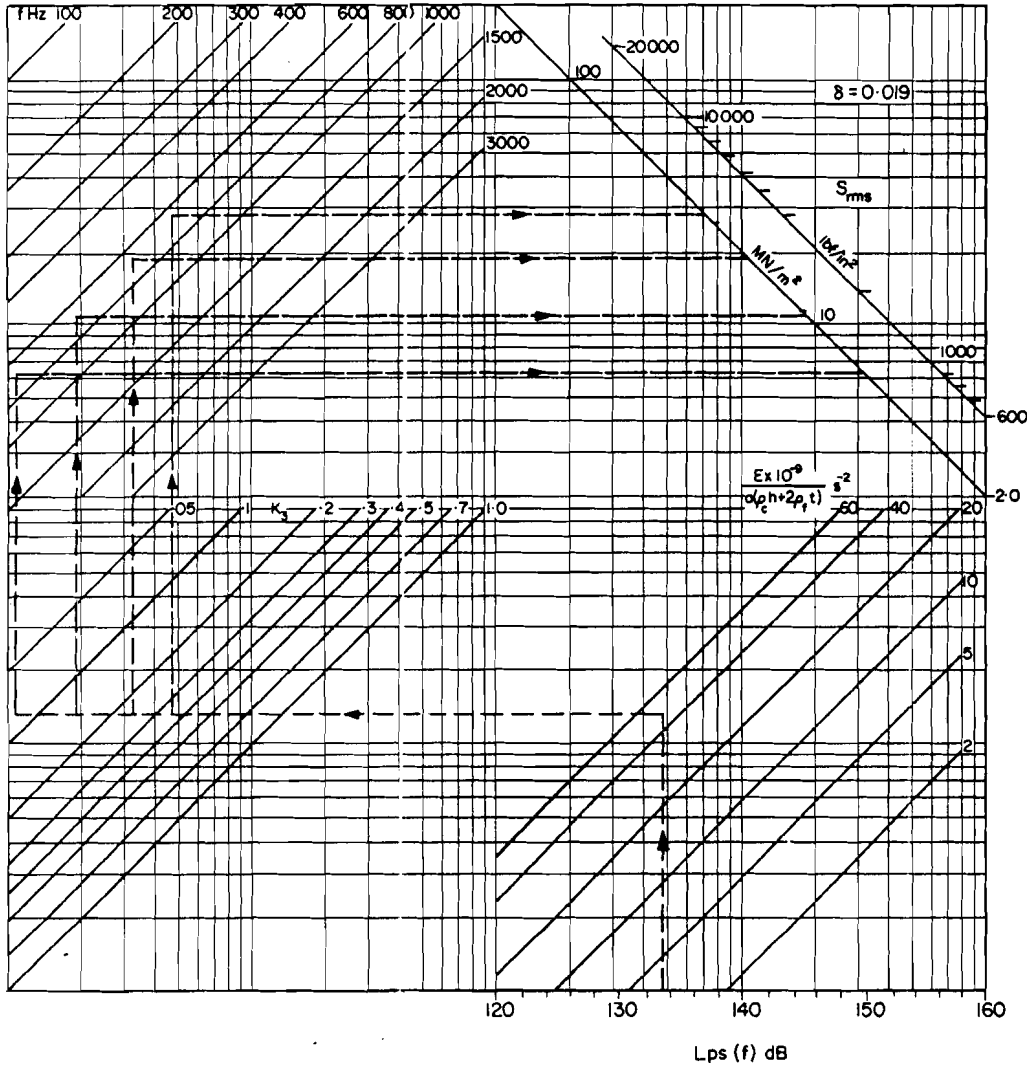


FIGURE 3.13. STRESS NOMOGRAPH

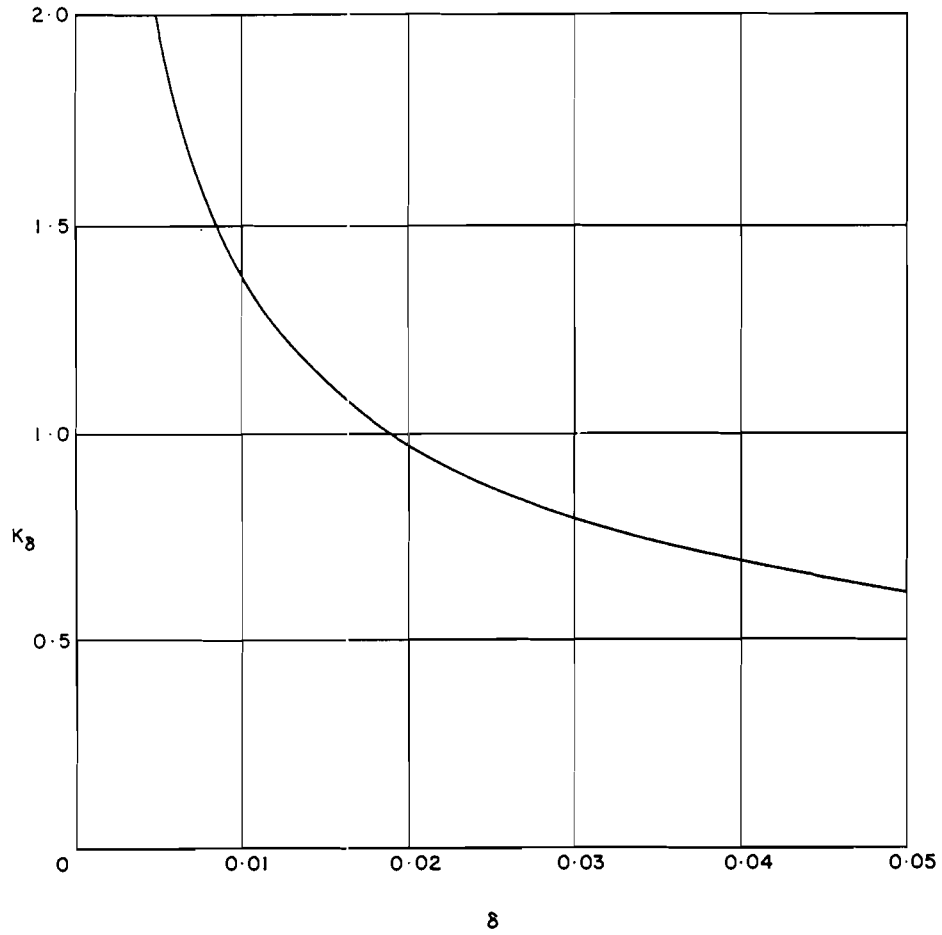


FIGURE 314. DAMPING RATIO CORRECTION FACTOR

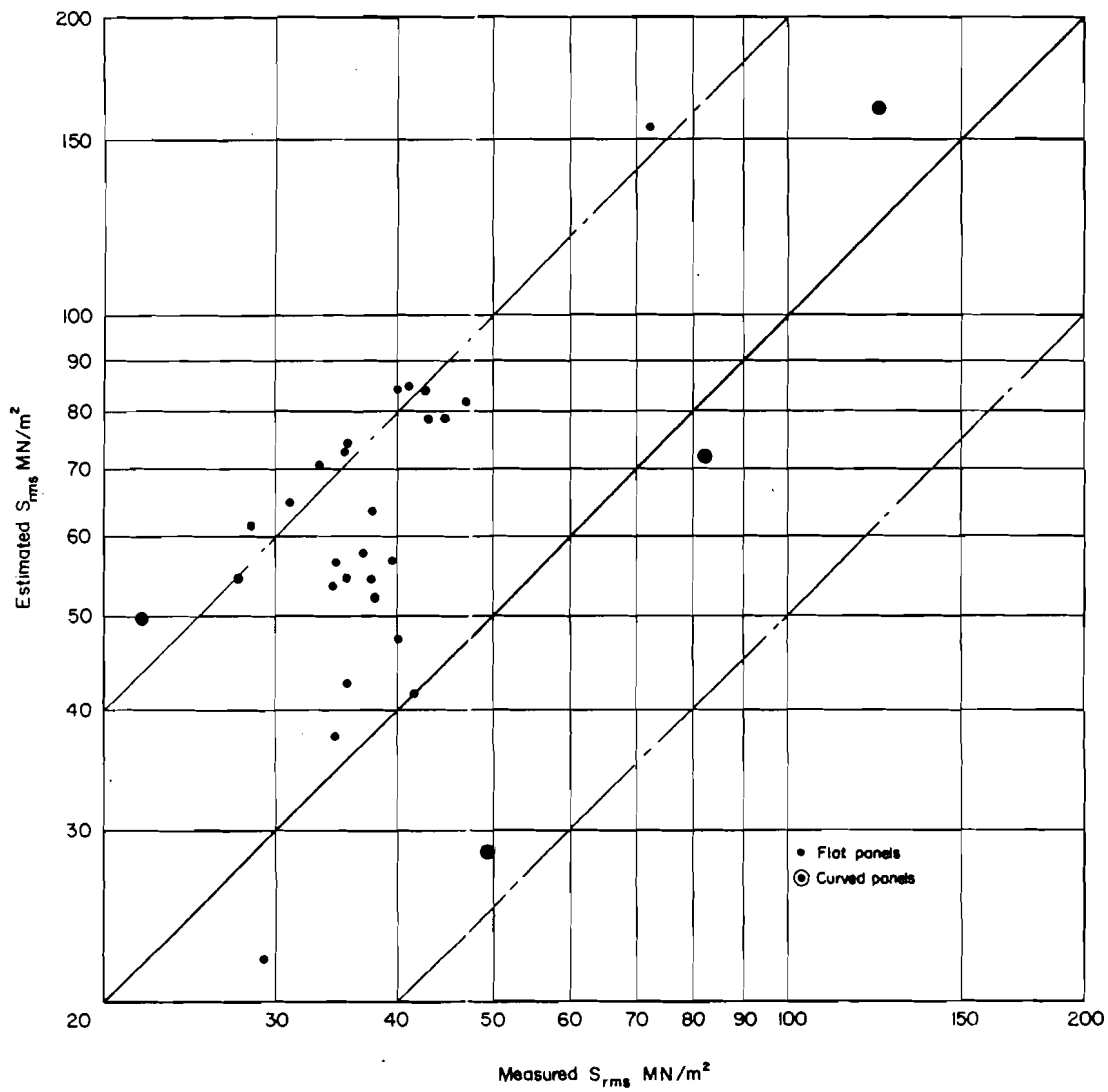


FIGURE 3.15. COMPARISON OF ESTIMATED AND MEASURED STRESS USING CALCULATED FREQUENCY AND  $\delta = 0.019$  FOR STRESS ESTIMATION

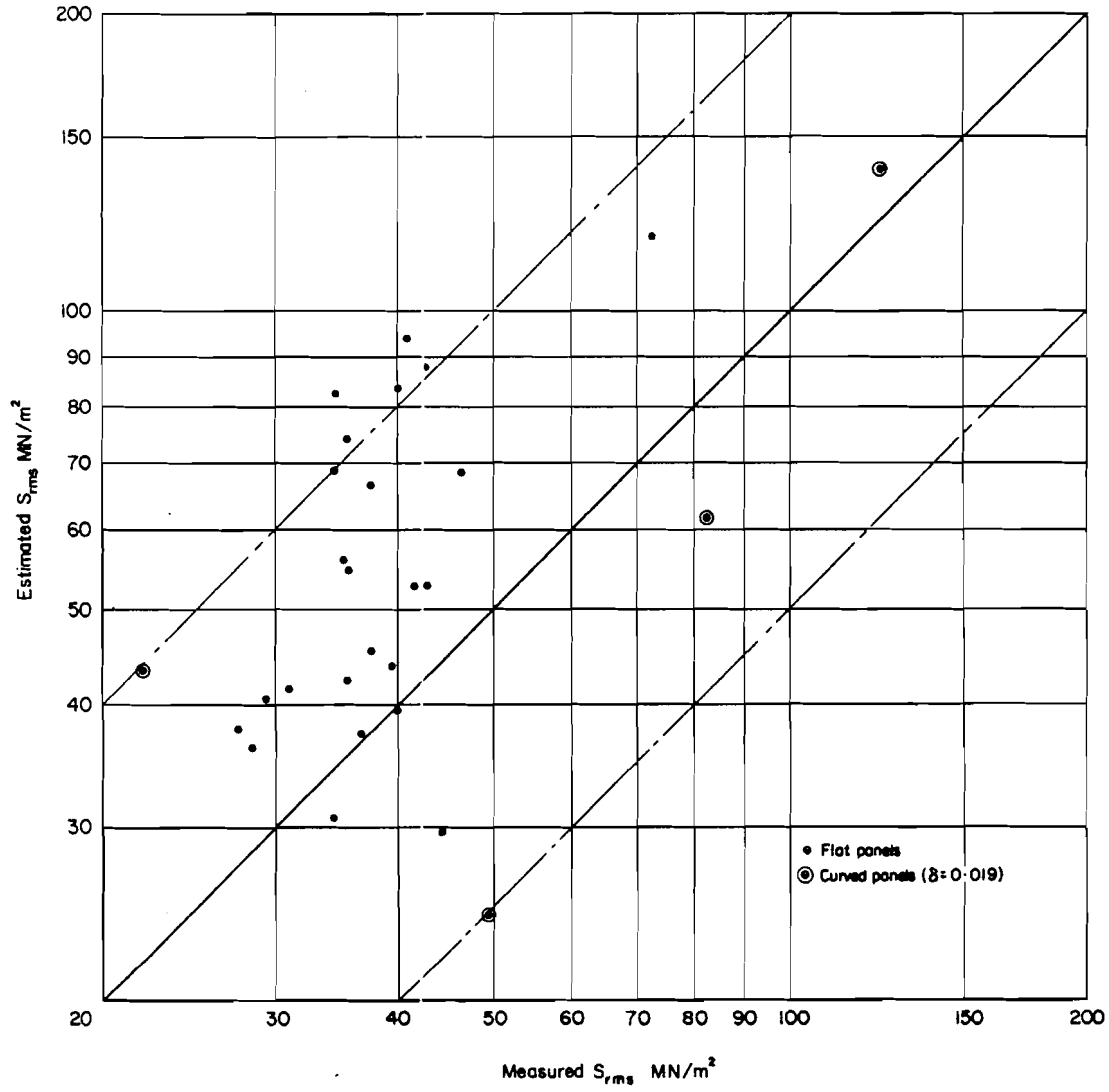


FIGURE 3.16. COMPARISON OF ESTIMATED AND MEASURED STRESS USING MEASURED FREQUENCY AND DAMPING FOR STRESS ESTIMATION

APPENDIX 3A  
COMPUTER PROGRAM

3A.1 General Notes

The first few natural frequencies and r.m.s. skin stresses of a singly curved sandwich panel may be found using this computer program. The assumptions given in paragraph 3.2 are applicable to the program.

A listing of instructions for two sub-programs is given in FORTRAN IV programming language. A main program is required to read in data and print out calculated values of natural frequency and r.m.s. skin stress. A listing of instructions for this program is not given as the instructions required are dependent on the particular computer used. The requirements for the main program are given in the form of a flow chart Figure 3A.1 and details of the sub-programs are given below.

The main program must include the COMMON statement which is written in both the frequency and stress sub-programs.

When run on a CDC 6600 computer, with suitable main program to read in data and print out frequencies and stresses, 16K store was used and the execution time for six sets of panel data was less than one second.

3A.2 Frequency Sub-Program

This sub-program solves for all natural frequencies where there are not more than three half-waves in either direction across the panel. The panel edges are assumed to be simply-supported.

The panel frequency data to be input for each panel considered are values for the variables listed in Table 3A.1.

TABLE 3A.1

VARIABLE	VARIABLE NAME	VARIABLE	VARIABLE NAME
a	A	$G_a$	GA
b	B	$G_b$	GB
h	H	E	E
t	T	$\rho_c$	RHOC
$R^*$	R	$\rho_f$	RHOF

\* For flat panels input dummy negative value for R.

Any coherent set of units in which time is expressed in seconds may be used, the frequencies being obtained in Hz.

On returning to the main program from the frequency sub-program the natural frequencies of the panel are stored in ARRAY F as shown in Table 3A.2. In this table m is the number of half waves across the panel in the direction parallel to the side of length a, and n is the number of half waves across the panel in the direction parallel to the side of length b.

TABLE 3A.2

$m \backslash n$	1	2	3
1	F(1,1)	F(1,2)	F(1,3)
2	F(2,1)	F(2,2)	F(2,3)
3	F(3,1)	F(3,2)	F(3,3)

### 3A.3 Stress Sub-Program

This sub-program solves for the r.m.s. face-plate stresses at the centre of a sandwich panel. The panel edges are assumed to be simply-supported.

The panel stress data to be input for each stress case considered are values for the variables listed in Table 3A.3.

TABLE 3A.3

VARIABLE	VARIABLE NAME
$L_{ps}(f)$	SPL
$\delta$	DELTA

In this sub-program the r.m.s. fluctuating pressure equivalent to  $L_{ps}(f)$  is computed. The units of this pressure in the sub-program are  $N/m^2$ . If British units are used this pressure must be calculated in units of  $lb/in^2$ . To obtain this pressure in British units the statement against label 110 should be replaced by

```
X2 = 10.0 ** (SPL/20.0 - 8.53749).
```

On returning to the main program from the stress sub-program the r.m.s. face-plate stresses are stored in ARRAY STR as shown in Table 3A.4

TABLE 3A.4

	Parallel to side a	Parallel to side b	Resultant
Inner or concave face-plate stress	STR(1,1)	STR(1,2)	STR(1,3)
Outer or convex face-plate stress	STR(2,1)	STR(2,3)	STR(2,3)

SUBROUTINE FOR SANDWICH PANEL FREQUENCIES (ALL EDGES SIMPLY-SUPPORTED)

```

SUBROUTINE FREQ
COMMON A,B,E,GA,GB,R,T,F(3,3),RHOF,RHOC,SPL,DELTA,STR(2,3),H
PNU=0.3
C
C CALCULATE SANDWICH PANEL NATURAL FREQUENCIES
C
DO 101 N=1,3
DO 101 M=1,3
XT=GA*A**2*H*(1.0-PNU**2)/(15.303*E*T*(T+H)**2)/M**2
XF=(A*N/(M*B))*(1.0+PNU)**2-(2.0*(A*N/(M*B))**2+1.0-PNU)*(2.0+
1*(A*N/(M*B))**2*(1.0-PNU))
XJ=39.478*GB/GA+6.2832/XT*(2.0*(A*N/(M*B))**2+1.0-PNU+GB/GA*(2.0+
1*(A*N/(M*B))**2*(1.0-PNU))-XF/XT**2
XK3=(-19.739/(A*XJ))*(6.2832*GB/GA+(2.0*(A*N/(M*B))**2+1.0-PNU-
1GB/GA*(A*N/(M*B))**2*(1.0+PNU))/XT)
XK4=(-19.739/(A*XJ))*(6.2832*A*N*GB/(M*B*GA)+(A*N*GB/(M*B*GA))*(2.0
1*(A*N/(M*B))**2*(1.0-PNU))-A*N/(M*B)*(1.0+PNU))/XT)
X=XT*(A*XK3+GB*A**2*N*XK4/(M*B*GA)+3.1416*(1.0+(A*N/(M*B))**2*GB/
1GA))
IF(R)102,102,103
C
C CALCULATE CURVATURE FACTOR
C
103 XK1=A/(1.5708*R*XF)*((A*N/(M*B))**2*(1.0+PNU)-PNU*(2.0*(A*N/(M*B))
1**2+1.0-PNU))/M
XK2=A/(1.5708*R*XF)*(PNU*(1.0+PNU)-2.0-(A*N/(M*B))**2*(1.0-PNU))/M
X=X+(A**2/(4.9348*(H+T)*R))**2*(1.0-(3.1416*R/A)*(A*N/(M*B)*XK2+
1PNU*XK1))/M**2
102 THETA=SQRT(X)
101 F(M,N)=3.1416*THETA/A**2*SQRT(E*T*(T+H)**2/(8.0*(1.0-PNU**2)*(RHOC
1*H+2.0*RHOF*T)))*M**2
RETURN
END

```

SUBROUTINE FOR SANDWICH PANEL FACE-PLATE R.M.S. STRESSES

```

SUBROUTINE STRESS
COMMON A,B,E,GA,GB,R,T,F(3,3),RHOF,RHOC,SPL,DELTA,STR(2,3),H
PNU=0.3
C
C CALCULATE RMS STRESS
C
XF1=(A/B*(1.0+PNU))**2-(2.0*(A/B)**2+1.0-PNU)*(2.0+(A/B)**2*(1.0-
1PNU))
XF2=4.0*3.14159**2*GB/GA+E*T*(T+H)**2*3.14159**4/(GA*A**2*H*(1.0-
1PNU**2))*(2.0*(A/B)**2+1.0-PNU+GB/GA*(2.0+(A/B)**2*(1.0-PNU)))-
2XF1/(2.0*GA*A**2*H*(1.0-PNU**2))/(3.14159**3*E*T*(T+H)**2)**2
XK3=6.28318*GB/GA+(2.0*(A/B)**2+1.0-PNU-GB/GA*(A/B)**2*(1.0+PNU))/
1(GA*A**2*H**2.0*(1.0-PNU**2))*(E*T*(T+H)**2*3.14159**3)
XK4=6.28318*A/B*GB/GA+(A/B*GB/GA*(2.0+(A/B)**2*(1.0-PNU))-PNU*(1.0
1+PNU))/(GA*A**2*H**2.0*(1.0-PNU**2))*(E*T*(T+H)**2*3.14159**3)
XK2A=-2.0*3.14159**3/XF2*(XK3+PNU*A/B*XK4)
XK2B=-2.0*3.14159**3/XF2*(PNU*XK3+A/B*XK4)
X1=(0.019/DELTA)**0.5
110 X2=10.0*(SPL/20.0-4.69897)
X=14.51*X1*X2*E*(F(1,1))**(-1.5)/((1.0-PNU**2)*3.14159**3.5*A*(
1RHOC*H+2.0*RHOF*T))
XK1=(A/B)**2*(1.0+PNU)-PNU*(2.0*(A/B)**2+1.0-PNU)
XK2=PNU*(1.0+PNU)-2.0-(A/B)**2*(1.0-PNU)
XK1A=-2.0/XF1*XK1+PNU-2.0/XF1*XK2*PNU*A/B
XK1B=-2.0/XF1*XK2*A/B+1.0-2.0/XF1*XK1*PNU
IF(R)111,111,112
111 X1=0.0
GO TO 113
112 X1=A/R
113 X2=(H/2.0+T)/A
STR(1,1)=X*ABS(X1*XK1A-X2*XK2A)
STR(2,1)=X*ABS(X1*XK1A+X2*XK2A)
STR(1,2)=X*ABS(X1*XK1B-X2*XK2B)
STR(2,2)=X*ABS(X1*XK1B+X2*XK2B)
STR(1,3)=SQRT((STR(1,1))**2+(STR(1,2))**2)
STR(2,3)=SQRT((STR(2,1))**2+(STR(2,2))**2)
RETURN
END

```

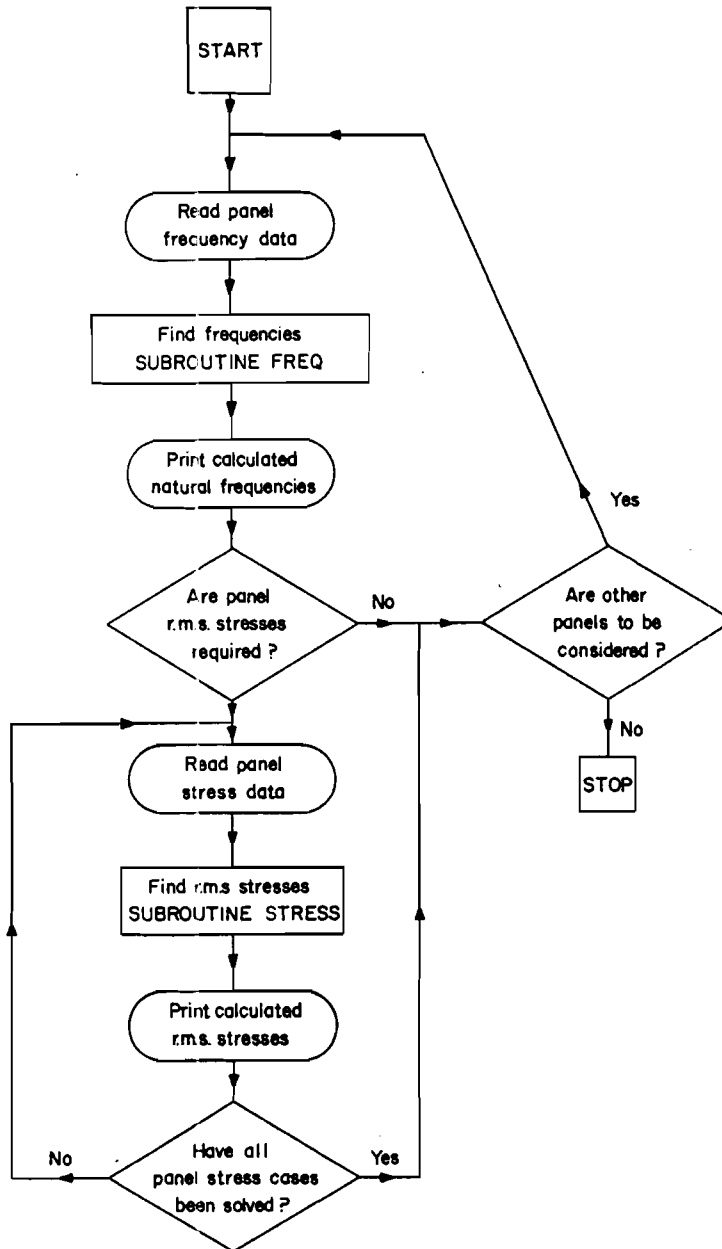


FIGURE 3A.I. COMPUTER PROGRAM FLOW CHART

## NATIONAL DISTRIBUTION CENTRES FOR UNCLASSIFIED AGARD PUBLICATIONS

Unclassified AGARD publications are distributed to NATO Member Nations through the unclassified National Distribution Centres listed below

### BELGIUM

Coördinateur AGARD – V.S.L.  
Etat-Major Forces Aériennes  
Caserne Prince Baudouin  
Place Dailly, Bruxelles 3

### CANADA

Director of Scientific Information Services  
Defence Research Board  
Department of National Defence, – 'A' Building  
Ottawa, Ontario

### DENMARK

Danish Defence Research Board  
Østerbrogades Kaserne  
Copenhagen Ø

### FRANCE

O.N.E.R.A. (Direction)  
29, Avenue de la Division Leclerc  
92, Châtillon-sous-Bagneux

### GERMANY

Zentralstelle für Luftfahrt-dokumentation  
und Information  
Maria-Theresia Str. 21  
8 München 27

### GREECE

Hellenic Armed Forces Command  
D Branch, Athens

### ICELAND

Director of Aviation  
c/o Flugrad  
Reykjavik

### ITALY

Aeronautica Militare  
Ufficio del Delegato Nazionale all'AGARD  
3, Piazzale Adenauer  
Roma/EUR

### LUXEMBOURG

Obtainable through BELGIUM

### NETHERLANDS

Netherlands Delegation to AGARD  
National Aerospace Laboratory, NLR  
P.O. Box 126  
Delft

### NORWAY

Norwegian Defense Research Establishment  
Main Library,  
P.O. Box 25  
N-2007 Kjeller

### PORTUGAL

Direccao do Servico de Material  
da Forca Aerea  
Rua de Escola Politecnica 42  
Lisboa  
Attn of AGARD National Delegate

### TURKEY

Turkish General Staff (ARGE)  
Ankara

### UNITED KINGDOM

Defence Research Information Centre  
Station Square House  
St. Mary Cray  
Orpington, Kent BR5 3RE

### UNITED STATES

National Aeronautics and Space Administration (NASA)  
Langley Field, Virginia 23365  
Attn: Report Distribution and Storage Unit

\* \* \*

If copies of the original publication are not available at these centres, the following may be purchased from:

#### *Microfiche or Photocopy*

National Technical  
Information Service (NTIS)  
5285 Port Royal Road  
Springfield  
Virginia 22151, USA

#### *Microfiche*

ESRO/ELDO Space  
Documentation Service  
European Space  
Research Organization  
114, Avenue Charles de Gaulle  
92200, Neuilly sur Seine, France

#### *Microfiche*

Technology Reports  
Centre (DTI)  
Station Square House  
St. Mary Cray  
Orpington, Kent BR5 3RE  
England

The request for microfiche or photocopy of an AGARD document should include the AGARD serial number, title, author or editor, and publication date. Requests to NTIS should include the NASA accession report number.

Full bibliographical references and abstracts of the newly issued AGARD publications are given in the following bi-monthly abstract journals with indexes:

Scientific and Technical Aerospace Reports (STAR)  
published by NASA,  
Scientific and Technical Information Facility,  
P.O. Box 33, College Park,  
Maryland 20740, USA

United States Government Research and Development  
Report Index (USGDR), published by the  
Clearinghouse for Federal Scientific and Technical  
Information, Springfield, Virginia 22151, USA

